Baseline monitoring at Wallooskee-Youngs restoration site, 2015: Blue carbon and channel morphology




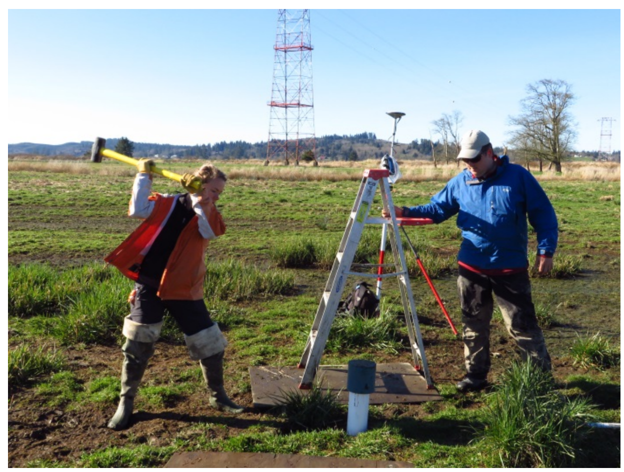

March 11, 2016

Prepared by:
Laura S. Brophy, Laura A. Brown, Michael J. Ewald, and Erin K. Peck
Estuary Technical Group, Institute for Applied Ecology, Corvallis, Oregon

Prepared for:
Lower Columbia Estuary Partnership, Portland, Oregon

Institute for Applied Ecology

Baseline monitoring at Wallooskee-Youngs restoration site, 2015: Blue carbon and channel morphology

Authors:
Laura S. Brophy, Laura A. Brown, Michael J. Ewald, and Erin K. Peck

Institutional affiliations for authors:
Estuary Technical Group, Institute for Applied Ecology, Corvallis, Oregon

Contact information for lead author:
Laura Brophy, Director, Estuary Technical Group of the Institute for Applied Ecology, brophyonline@gmail.com, (541) 752-7671

Recommended citation:
Brophy, L.S., L.A. Brown, M.J. Ewald, and E.K. Peck. 2015. Baseline monitoring at Wallooskee-Youngs restoration site, 2015: Blue carbon and channel morphology. Corvallis, Oregon: Institute for Applied Ecology.

Data availability: Data from this project are available from the lead author listed above.

Acknowledgments:

- We are grateful for the funding provided for this project by the Bonneville Power Administration through the Lower Columbia Estuary Partnership and by US Fish and Wildlife Service through a National Fish Passage Program grant.
- We thank Rudy Salakory and the Cowlitz Indian Tribe for coordination, site access, and technical input for this project.
- We thank the Columbia River Estuary Study Taskforce (CREST) for its major contribution to this project through the loan of a boat and field assistance from April Silva and Narayan Elasmar.
- We thank Oregon State University and Dr. Rob Wheatcroft for the use of facilities and assistance with the carbon coring and analysis.
- Many thanks to those who assisted with field data collection: David Beugli, Issac Kentta and Sarah Kidd.

Table of contents

Summary and key findings

This report describes results from baseline monitoring of coastal “blue carbon” (carbon stored in soils of coastal wetlands) and channel morphology at the Wallooskee-Youngs restoration site and reference sites in the Youngs Bay estuary. This work, conducted by the Estuary Technical Group (ETG) at the Institute for Applied Ecology, was funded through a contract between ETG and the Lower Columbia Estuary Partnership (LCEP).

During 2015, ETG, working in collaboration with a team from Oregon State University led by Dr. Rob Wheatcroft, collected and began to analyze carbon cores from the Wallooskee-Youngs restoration site and two nearby reference sites (Daggett Point and Cooperage Slough). The information collected will allow us to quantify sediment and carbon accumulation rates at the reference sites, estimate carbon losses that occurred when the restoration site was diked and drained, and predict post-restoration carbon accumulation rates at the restoration site. Carbon core analysis is still in progress under separate funding from the U.S. Fish and Wildlife Service (USFWS); a final report will be issued in at the end of 2016.

Under this contract with LCEP, ETG also collected and/or analyzed channel morphology data from Wallooskee-Youngs and four reference sites (Daggett Point, Cooperage Slough, Grant Island, and Fry Island). ETG generated a high-resolution channel network map at the reference sites using automated and consistent LIDAR-derived methods. ETG also analyzed channel cross-section data provided by Statewide Land Surveying for the Wallooskee-Youngs site, and conducted field measurements of channel cross-sections at two of the reference sites (Daggett Point and Cooperage Slough). The resulting channel morphology data are useful in interpreting the results of carbon accumulation measurements and other monitored parameters (as described below).

Under separate funding from the USFWS, ETG is also monitoring the following additional parameters at the Wallooskee-Youngs restoration site and the Daggett Point, Grant Island, and Cooperage Slough reference sites: tidal hydrology (surface water level), surface water salinity, groundwater level, groundwater salinity, and vegetation composition. The resulting data will help advance our understanding of the physical drivers behind carbon accumulation rates, complementing the blue carbon study. This monitoring (and ongoing analysis of carbon cores) will continue during 2016; a final report from this work will be produced at the end of 2016.

Key findings

Key findings for blue carbon:

- Sediment accretion rate has been calculated for one site (high marsh at the Daggett Point reference site). The rate was 0.35 cm yr^{-1}, which was consistent with preliminary estimates of sediment accretion in other portions of the reference site. This rate was also comparable to rates found in high marsh across the Pacific Northwest using the feldspar marker horizon method (Thom 1992).

- Cores are still in the process of being analyzed; complete results will be reported at the end of 2016. The report will include results from USFWS-funded monitoring of controlling factors for carbon accumulation, such as groundwater levels, tidal inundation regime, and salinity, as well as associated structural and biotic characteristics.

Key findings for channel morphology:

- Channel networks at four reference sites were extracted from LIDAR using a least-cost flow-routing algorithm that was calibrated against field data from Millport Slough in the Siuslaw River estuary (Siletz Bay National Wildlife Refuge).

- Based on LIDAR analysis, channel density was reduced by approximately 78% at Wallooskee-Youngs following conversion to agriculture. Channel density was 11 km/km^2 at Wallooskee-Youngs compared to 42-52 km/km^2 at reference sites.

- Our analysis indicated that reference tidal wetlands had many more outlets of first-order channels than previously documented or predicted.

- Channels at the Wallooskee-Youngs restoration site had a greater width-to-depth ratio (wider and shallower) compared to channels at least-disturbed reference sites.

- The largest (widest) channels at the Wallooskee-Youngs restoration site were shallower and had a higher flowpath elevation compared to similar-sized channels at the reference sites.

Study overview

This report describes results from baseline monitoring of coastal "blue carbon" (carbon stored in soils of coastal wetlands) and channel morphology at the Wallooskee-Youngs restoration site and reference sites in the Youngs Bay estuary. This work, conducted by the Estuary Technical Group (ETG) at the Institute for Applied Ecology, was funded through a contract between ETG and the Lower Columbia Estuary Partnership (LCEP). In this report we summarize the rationale, methods, results, discussion, and future plans for the blue carbon and channel morphology studies conducted in 2015.

During 2015, ETG, working in collaboration with a team from Oregon State University led by Dr. Rob Wheatcroft, collected and began to analyze carbon cores from the Wallooskee-Youngs restoration site and two nearby reference sites (Daggett Point and Cooperage Slough). The information collected will allow us to quantify carbon accumulation rates at the reference sites, estimate carbon losses that occurred when the restoration site was diked and drained, and predict post-restoration carbon accumulation rates at the restoration site. Carbon core analysis is still in progress under separate funding from the U.S. Fish and Wildlife Service (USFWS); a final report will be issued at the end of 2016 when analysis is complete.

Under this contract with LCEP, ETG also collected and/or analyzed channel morphology data from Wallooskee-Youngs and four reference sites (Daggett Point, Cooperage Slough, Grant Island, and Fry Island). ETG generated a high-resolution channel network map at the reference sites using automated and consistent LIDAR-derived methods. ETG also analyzed channel cross-section data provided by Statewide Land Surveying for the Wallooskee-Youngs site, and conducted field measurements of channel cross-sections at two of the reference sites (Daggett Point and Cooperage Slough). The resulting channel morphology data are useful in interpreting the results of carbon accumulation measurements and other monitored parameters (as described below).

Under separate funding from the USFWS, ETG is also monitoring the following additional parameters at the Wallooskee-Youngs restoration site and the Daggett Point, Grant Island, and Cooperage Slough reference sites: tidal hydrology (surface water level), surface water salinity, groundwater level, groundwater salinity, and vegetation composition. The resulting data will help advance our understanding of the physical drivers behind carbon accumulation rates, complementing the blue carbon study. This monitoring (and ongoing analysis of carbon cores) will continue in 2016; a final report from this work will be produced at the end of 2016.

Youngs Bay estuary study sites

We investigated carbon accumulation and channel morphology at the Wallooskee-Youngs restoration site and four least-disturbed tidal wetland reference sites located in the Youngs Bay estuary (Figure 1). Site characteristics were summarized in Table 1. The Wallooskee-Youngs site was not yet restored, so all data from the Wallooskee-Youngs site presented in this report represent pre-restoration (baseline) data.

The Wallooskee-Youngs restoration site is a 193.11 acre site at the confluence of the Wallooskee River and Youngs Bay (Figure 1). The site was used as a dairy farm for 80 years prior to 2011, when dairy operations stopped. The site has been ditched, tiled, seeded and grazed. Restoration will be accomplished through grading and excavation of channels, tidegate removal, and levee lowering and breaching, in order to restore tidal influence to the site. The restoration of this site is sponsored by the Cowlitz Indian Tribe.

Four least-disturbed reference sites provided examples of pre-disturbance conditions and goals for a restoration trajectory at the Wallooskee-Youngs restoration site. Reference sites were selected to represent historic conditions that were likely present at Wallooskee-Youngs prior to diking and conversion to agricultural use. Reference site selection was also based on proximity and similar geomorphic setting to Wallooskee-Youngs, and along a salinity gradient to get a full range of the physical drivers for carbon accumulation. These similarities and differences will help interpret post-restoration changes in carbon drivers at Wallooskee-Youngs by providing a “before-after-control-impact” (BACI) statistical framework – optimal for restoration effectiveness monitoring (Stewart-Oaten 1986, 1992), and by allowing a gradient of physical drivers to determine effects on carbon accumulation.

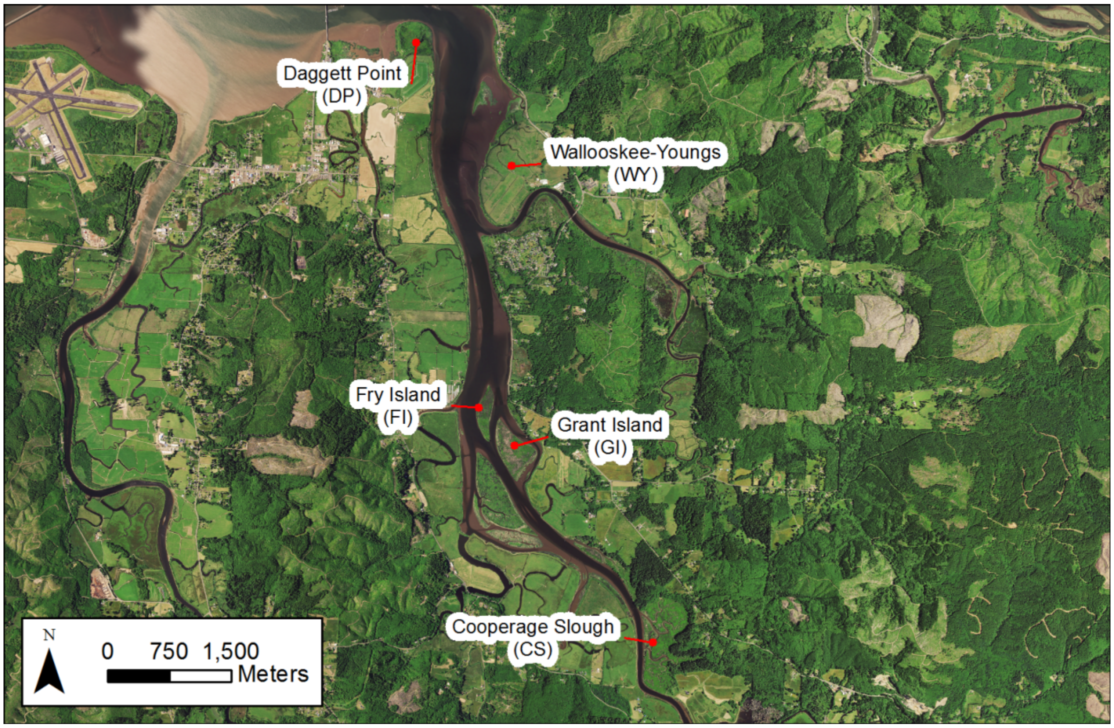

Figure 1. Overview of the study sites in the Youngs Bay estuary, Oregon. Background: NAIP 2014.

Table 1. Site descriptions for Youngs Bay estuary reference sites. River miles were calculated using the Oregon DEQ RM Calculator (http://deqgisweb.deq.state.or.us/llid/llid.html).

Site	**Wallooskee-Youngs (WY)**	**Daggett Point (DP)**	**Fry Island (FI)**	**Grant Island (GI)**	**Cooperage Slough (CS)**
River mile	1.98	0.63	3.89	4.24	6.60
Site type	Pre-restoration	Reference	Reference	Reference	Reference
Historic wetland type (1850s)*	Tidal marsh; Sitka spruce or crabapple may be included on higher parts of site.	Tidal marsh; Sitka spruce or crabapple may be included on higher parts of site.	Tidal marsh; Sitka spruce or crabapple may be included on higher parts of site.	Tidal marsh; Sitka spruce or crabapple may be included on higher parts of site.	Sitka spruce swamp; combinations of willow, red alder, red cedar, hemlock; Dense understory may include salmonberry, crabapple, elderberry, gooseberry, briers, ferns, skunk cabbage, and vine maple.
Alterations, impacts	Diking, ditching, grazing, tree and shrub removal	Power transmission tower, potential dredging of large channel	Possible grazing	Enhanced and natural levee/dike, possible grazing	No known alterations

Channel condition	Ditched	Natural, meandering, one possible excavated large channel	Natural, meandering	Natural, meandering	Natural, meandering

* from Hawes *et al.* (2008)

Sediment and "blue" carbon accumulation

Background

Sediment and soil carbon ("blue" carbon) accumulation rates will be quantified at the Wallooskee-Youngs tidal wetland restoration site, and compared to nearby least-disturbed tidal wetland reference sites (Daggett Point and Cooperage Slough) to establish the soil carbon losses that occurred when the restoration sites were diked and drained. This information will additionally allow prediction of the carbon sequestration capacity of restored tidal wetlands, which is likely substantial for tidal wetlands in the Pacific Northwest (Crooks *et al.* 2013). These goals will be accomplished through measurement of soil carbon stocks by analysis of carbon content and bulk density of sediment within cores collected from both restoration and reference sites. Soil carbon accumulation rates will be calculated using the soil carbon concentration data in addition to sediment accumulation rates, obtained by ^{210}Pb and ^{137}Cs analysis.

Methods

Field techniques and sample preparation

Within the restoration site, Wallooskee-Youngs, three 1.5-m-long cores were collected, and within each of the two associated reference sites, Daggett Point and Cooperage Slough, two 3-m and one 1.5-m-long cores were collected. Coring locations were selected based on field reconnaissance and review of available data, including elevation, aerial photographs, vegetation, and soil survey maps. Coring included driving cores into the sediment and retrieval through use of a truck jack. In the field each long core was cut into two ~1.5-m-long sections using a pipe cutter. These sections were transported to OSU in an upright position and are stored within the OSU Marine Geology Repository's refrigerated core storage facility.

Soon after collection, all core sections were scanned using a Computerized Tomography (CT) system at the OSU College of Veterinary Medicine. CT imaging provides high-resolution views of sediment stratigraphy that includes physical and biogenic sedimentary structures, and estimates of sediment bulk density. The top (~50 cm) of each core was sectioned vertically at 2-cm increments, and the samples freeze dried for 48 hr, removing all water.

Radionuclides

Assuming a constant deposition rate and a relatively unmixed profile, the exponential decrease in excess ^{210}Pb activity with depth and the known decay rate of ^{210}Pb provide an estimate of sediment accumulation rate within the wetland. ^{137}Cs, primarily deposited as fallout from atmospheric nuclear weapons testing, provides an additional estimate of the sediment accumulation rate, assuming its deposition started when weapons testing commenced in 1954. Samples were prepared by first removing large pieces of plant material from the dried sediment, then grinding the sample to a constant consistency using a mortar and pestle. Approximately 20 – 40 g of material were weighed into jars and the volume of the compacted and leveled sediment was recorded. Each sample was counted for ≥24 hr on two equivalent Canberra gamma detectors and the activities of the radionuclides ^{210}Pb, ^{214}Pb, and ^{137}Cs were measured at their respective photopeaks (46.5, 352.0, and 661.6 keV) (Wheatcroft and Sommerfield 2005).

Carbon content

Analyzed with sediment accumulation rates, sediment carbon concentrations allow us to quantify carbon accumulation rates within each restoration site and the nearby least-disturbed reference sites. This provides an estimate of carbon losses when the restoration site was diked and drained and a prediction of the post-restoration carbon sequestration capacity of these sites. Loss on ignition (LOI) will be used to measure organic matter content within the sediment samples and a relationship between organic matter and organic carbon content will additionally be measured in a subset of samples using an automated elemental analyzer (CHN analyzer). The LOI technique consists of weighing the freeze-dried sediment before and after combustion in a muffle furnace at ~550 °C for 4-8 hr (Heiri *et al.* 2001). The CHN method consists of packaging ~150 mg of dried sediment into a tin capsule, followed by analysis by the instrument (Howard *et al.* 2014).

Preliminary results

The following provides a preliminary interpretation of one core (core ID DP02L) from the high marsh of Daggett Point, and illustrates the types of information that can be obtained. Eventually similar interpretations will be provided for all cores, although interpretation may be more challenging for some samples. The CT image reveals bioturbated (i.e., mixed) organic-rich marsh sediment within the top portion of the core, and a gradual transition to a section with more sediment layering (bedding) (Figure 2). Such a transition likely reflects a decrease in sediment accumulation rates or a change of depositional environment from low to high marsh. At 124 cm there is a likely tsunami deposit that consists of a 6-cm-thick sandy section that has abundant physical sedimentary structures and a sharp lower contact with some rip-up clasts (small areas of muddy material). The sedimentary structures, rip-up clasts, and sharp contact all suggest rapid deposition of coarse sediment under high-energy conditions. It is likely that this deposit was formed by the last large Cascadia earthquake that occurred in 1700.

Sediment accumulation within the upper portion of this core (representing roughly a century of time) was calculated using the exponential decrease in excess ^{210}Pb activity with depth, indicated by the slope in Figure 3, and the known decay rate of ^{210}Pb. By this method, sediment accumulates at a rate of 0.35 cm yr^{-1} (R^2 = 0.98) within the high marsh at Daggett Point. This value is consistent with preliminary estimates of sediment accumulation rates within other portions of the reference site. The break in the excess ^{210}Pb profile at -35 cm likely results from a change in sediment grain size, as degree of radionuclide adsorption to particles is a result of the material's ratio of surface area to volume (i.e., particles with large surface-area-to-volume ratios experience greater radionuclide adsorption). Sediment grain size analysis will be used to investigate this possibility, as there is no evidence of a change in bedding in the CT image (Figure 2). The sediment accumulation rate calculated using the excess ^{210}Pb activity between -37 and -45 cm was 0.28 cm yr^{-1} (R^2 value of 0.98).

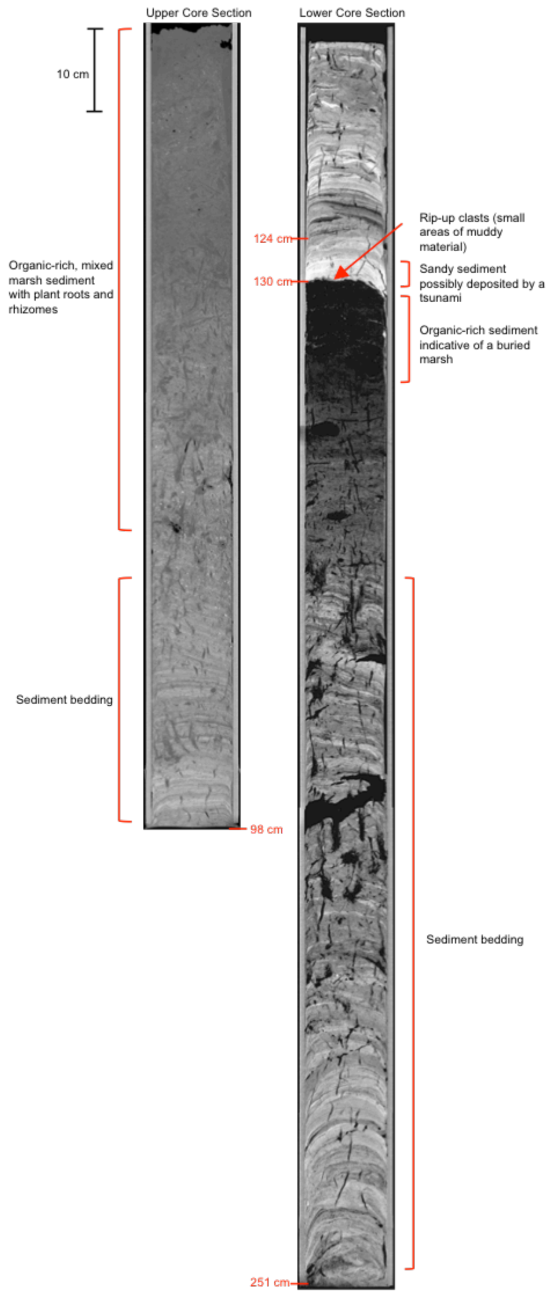

Figure 2. A negative CT image of the upper and lower sections of a 251-cm core collected in the high marsh at Daggett Point (core ID DP02L). Lighter colors indicate X-ray opaque materials, such as sand or shells, whereas darker materials denote X-ray transparent materials such as roots, bulk organic matter, or voids. Black indicates an absence of material.

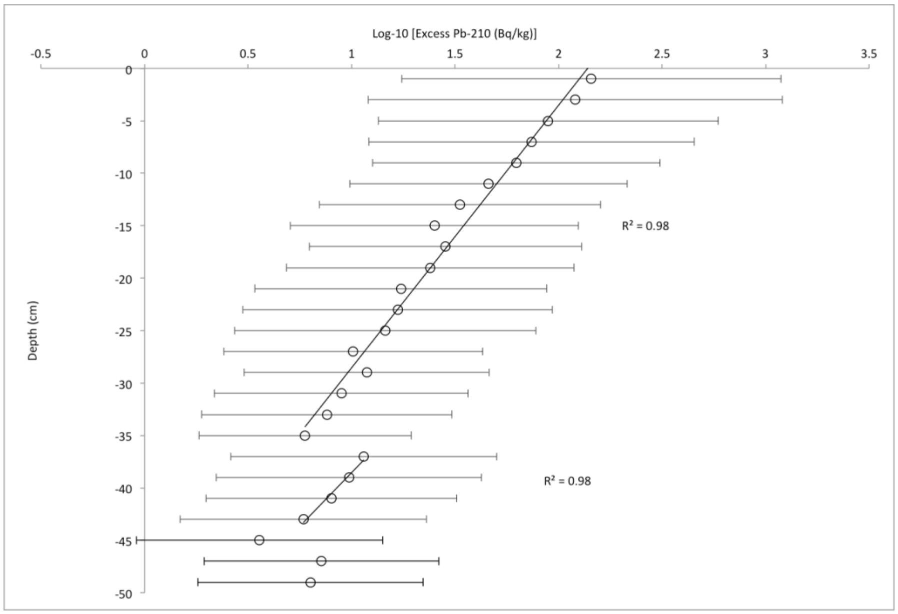

Figure 3. Excess ^{210}Pb within the top 50 cm of DP02L (carbon core located in high marsh at Daggett Point). Error bars indicate the log transformed standard error.

Future plans

In addition to analyzing the remaining gamma detection samples and quantifying the carbon content of the material, sediment grain size measurements will be made on a subset of core horizons using a laser particle size analyzer. Combined, these measurements will be used to characterize the quantity and type of organic carbon, and calculate the rate of sediment accumulation and carbon burial at each site. Using data from all cores collected, sediment and soil carbon accumulation rates will be compared between the Wallooskee-Youngs restoration site and the reference sites, and an estimate will be made of the soil carbon losses that occurred when the restoration site was diked and drained. Finally, the above information will be used to predict the carbon sequestration capacity of the restored Wallooskee-Youngs site.

Channel morphology

Introduction

During 2015, ETG analyzed field-based pre-restoration channel cross-section measurements for the Wallooskee-Youngs restoration site using data provided by Statewide Land Surveying (2012). ETG also developed and used a LIDAR-based channel mapping and morphology analysis method, and applied the method at four least-disturbed tidal wetland sites in the Youngs Bay estuary, Oregon. These reference sites were Daggett Point (DP), Fry Island (FI), Grant Island (GI), and Cooperage Slough (CS) (Figure 1, Table 1). As tidal forces are re-introduced to the Wallooskee-Youngs (WY) site following restoration, we expect to see the channel geometry shift towards equilibrium, following a trajectory towards the conditions currently present at the reference sites.

Other researchers have used remote methods to map tidal channel networks, establishing allometric models to describe natural systems and targets for channel restoration, (e.g., Diefenderfer *et al*. 2008; Hood 2002, 2004, 2007, 2014). Hood (2002) used aerial photography to digitize channel networks and relate slough channel length, width, area, and perimeter to wetland size in the Lower Chehalis River estuary, and made comparisons to a restored site. Hood also extended his work to establish these relationships within Puget Sound, Washington (Hood 2004, 2007) and the Lower Columbia (Hood 2014). Diefenderfer *et al*. (2008) used LIDAR data to relate channel cross-sectional area at the outlet to channel network features such as channel length, density, and catchment area for forested tidal wetland reference sites and restoration sites in the Lower Columbia. Additionally, the work of the Pacific Northwest National Laboratory and others has yielded impressive datasets describing conditions at restoration and least-disturbed reference sites in the Lower Columbia River estuary. Borde *et al.* (2011) conducted fieldwork to assess channel morphology, vegetation, sediment content, and inundation at 43 least-disturbed reference sites in the Lower Columbia River and estuary (LCRE), including Grant Island and Cooperage Slough.

Our effort was aimed at complementing the studies mentioned above and others in the Lower Columbia. The objective of our study was to provide a high-resolution rapid assessment of reference channel network characteristics in four least-disturbed sites near the Wallooskee-Youngs project, and to make comparisons between these reference site networks and the existing channel network at the Wallooskee-Youngs where appropriate. Two different approaches were used to achieve these objectives. The first approach was to map complete tidal channel networks using LIDAR and automated channel extraction software, calibrated to field data. Mapping complete channel networks enables comparisons of total channel length, channel density, and gradient. By tracking these metrics, inferences can be made between the current channel characteristics at the Wallooskee-Youngs site and its reference sites, and to highlight differences between reference sites. Since channel network density is generally much lower at diked sites compared to reference sites, tracking channel density after restoration can provide a very useful metric for site recovery (Williams *et al*. 2002).

ETG also developed a second approach meant to replicate field-based channel cross-sections using LIDAR. This approach yielded estimates of channel bankfull width (BFW), depth, width-to-depth ratio (WTD), and channel bank slope. BFW, depth, and WTD quantify habitat availability for salmonids and other wetland and aquatic species, allowing calculation of channel cross-sectional characteristics and therefore water volume flowing in and out of the site (tidal prism). While we developed an algorithm to automatically calculate these metrics from LIDAR, the underlying topographic data were too noisy for the algorithm to produce consistent and reliable estimates of BFW and depth. As a result, channel bank slope and WTD were also unreliable because they relied on accurate estimates of BFW and depth. We briefly describe our algorithm in the methods section below, but did not present the associated results. For more information, please contact the authors.

Our focus for this report builds on our experience at the Ni-les'tun restoration at Bandon Marsh National Wildlife Refuge on the Coquille River estuary of Oregon (Brophy *et al*. 2014) and the Waite Ranch restoration on the Siuslaw River estuary, Oregon (Brophy *et al.* 2015). At these project sites, we collected detailed, field-based channel cross-section measurements at restoration and reference sites to serve the purposes described above (effectiveness monitoring, quantification of the impact of site alterations, and data to help track system-wide changes due to large scale forces). While the methods used in Brophy *et al.* (2015a, 2015b) provided precise cross-sections, they are expensive to implement with a sample design that adequately measures channels of varying sizes with replication. Remote methods, such as the LIDAR method we have presented in this report, yield less-precise measurements at a cross-section or transect level, but offer the potential for very high spatial resolution at the site scale by yielding many replicates per channel size class across an entire channel network.

In addition to the LIDAR-based methods described above, we also made field measurements of channel cross-sectional characteristics at two of the reference sites (Daggett Point and Cooperage Slough). We compared these data to the channel survey data provided by Statewide Land Surveying for the Wallooskee-Youngs site.

Methods

LIDAR data and DEM generation

All analyses conducted for this report used the DOGAMI topographic LIDAR collected during late summer through fall of 2008 and 2009 (Watershed Sciences, Inc. 2009). LIDAR data collected in the summer may have considerable vegetation interference with the LIDAR signal; the magnitude of the effect depends on vegetation density and height, factors we were unable to quantify for the period of LIDAR acquisition. The LIDAR instrument and flight path parameters were structured to provide a minimum illuminated pulse spot size of between 15 cm and 40 cm, laser scan angle of less than ± 15 degrees, and greater than 50% side-lap (≥ 100% overlap) between opposing flight-lines to minimize the influence of laser shadowing and other artifacts (Watershed Sciences, Inc. 2009).

Using LIDAR in tidal wetlands poses many challenges. For example, vegetation may interfere with the LIDAR pulse, obscuring tidal channels and biasing elevation estimates by 10-15 cm depending on vegetation type (Montané and Torres 2006; Rosso *et al.* 2006; Sadro *et al.* 2007; Wang *et al.* 2009; Athearn *et al.* 2010; Chassereau *et al.* 2011; Schmid *et al.* 2011; Hladik and Alber,2012; Ewald 2013). In Oregon, Ewald (2013) found the difference between LIDAR-derived elevations and high-precision GPS/GNSS elevations to be between 10-15 cm in most high-marsh vegetation communities and 35-55 cm in slough sedge (*Carex obnupta*) and Lyngbye's sedge (*Carex lyngbyei*) communities. Unfortunately, the cattail/bulrush (*Typha*/*Schoenoplectus* spp.) community common at the reference sites was underrepresented in Ewald's study, and its typical interference was therefore not estimated in Ewald (2013).

Besides vegetation interference, geoprocessing steps like digital elevation model (DEM) generation, filtering approaches, and flow routing algorithms can significantly affect the outcome of LIDAR analysis (Bater and Coops 2009; Wehr and Lohr 1999; Meng *et al.* 2010). To address these potential challenges, we generated a new digital elevation model from the LIDAR point-cloud for each reference site using a minimum bin approach. The algorithm had a 2 m search radius and 1 m cell size (Ewald 2013). This method mitigates the effect of vegetation by selecting the lowest LIDAR return within 2 m of any given cell, while maintaining a high spatial resolution – and therefore the ability to resolve small features on the landscape such as channels (Ewald 2013). In addition, the minimum-bin approach is a simple filter-based DEM-generation technique that does not rely on assumptions about topographic shape or other features outside the search radius of the algorithm, and is therefore comparable between sites (Meng *et al.* 2010, Schmid *et al*. 2011).

Reference channel network extraction

Complete channel networks were rapidly delineated for the reference sites using an automated method that incorporates a D-infinity flow-accumulation algorithm coupled with least-cost routing approach to trace small depressions, such as channels (Tarboton 1997, Metz 2011). Channel network metrics including density, sinuosity, length, gradient, and order were then calculated for comparison among sites or among networks within each site. The underlying channel network extraction algorithm was implemented using a custom Python-based analysis framework that relies on the *r.stream* family of tools implemented within GRASS GIS 7.01 by Metz (2011). While these tools are intended for use within dendritic fluvial systems, they perform well in low-relief tidal topographies (Ewald and Brophy 2012). Unlike many other channel delineation techniques (e.g., ArcHydro, TauDem), least-cost approaches do not require a consistent slope between grid cells of a DEM nor "filling" sinks in the DEM. Therefore, the least-cost approach can overcome small dips and rises in the channel path if the route remains the least-expensive route in terms of "work" required to reach lower elevations in the DEM. The *r.stream* family of tools has been used successfully by our team in past studies to delineate and relate contiguous patches of current and former tidal-wetland for historic land-use classification and conservation/ restoration prioritization (Ewald and Brophy 2012). Small pits (i.e., < 2 m) in the DEM were removed using the *r.hydrodem* tool (Lindsay and Creed 2005).

The delineation tools required selection of an initialization threshold (the drainage area at which a channel is initiated and then cascaded downslope). Since we could not assume that initialization thresholds generated elsewhere would be appropriate, we generated our own initialization threshold by calibrating our analysis to field studies in similar wetlands on Oregon's outer coast. Specifically, we calibrated our channel network algorithm so that the resulting LIDAR-derived channel density matched the field-derived density from a complete field survey of channels at Millport Slough, a least-disturbed tidal marsh in the Siletz River estuary (So *et al.* 2009). The Siletz survey (So *et al.* 2009) constitutes the most complete tidal channel morphology dataset available for an Oregon tidal wetland. While it would have been ideal to calibrate our method using a complete channel survey in the Youngs Bay estuary, no such data were available, and generating them would have been well beyond the scope and budget of this project. The calibration process yielded an accumulation threshold of 176 pixels, equivalent to 147.2 m^2 drainage area at the point of channel initialization, yielding a channel density of 63.05 km/km^2 at the Millport Slough calibration site (Figure 4).

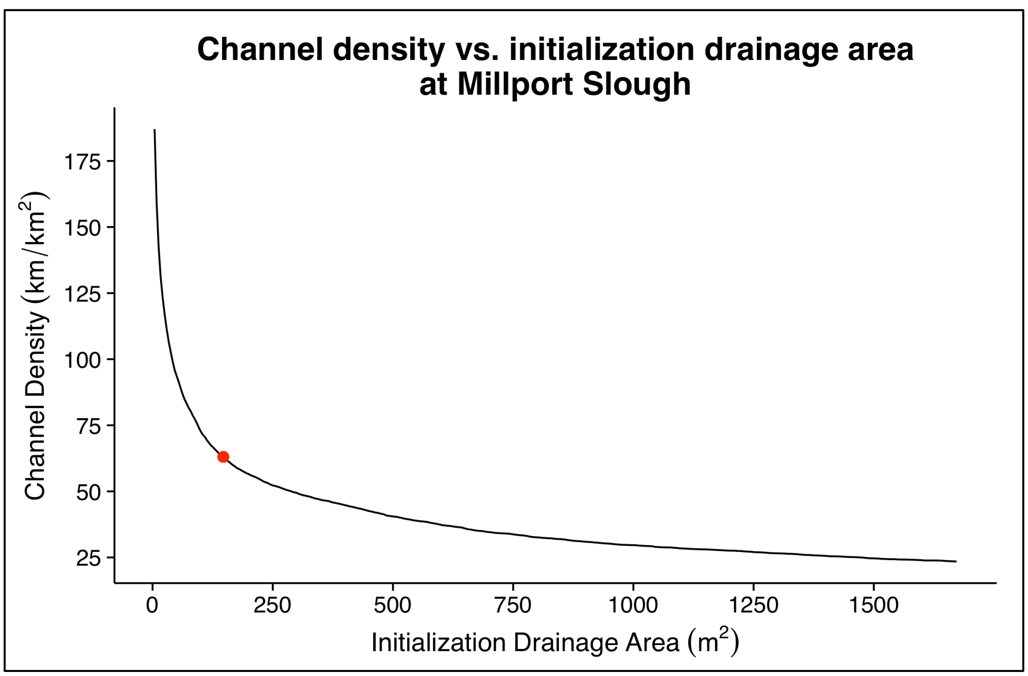

Figure 4. LIDAR-derived channel density vs. channel initialization drainage area at Millport Slough, Siuslaw River estuary, Oregon. The red dot is the field-calibrated initialization area (drainage area of

147.2 m^2) used in this study, selected because it is the value at which the LIDAR-derived density matches the field-mapping-derived channel density of 63.05 km/km^2.

The resulting channel network contained significant high-frequency noise as a result of the small-cell-size (*i.e.*, high spatial resolution) DEM. Therefore, the extracted channel networks were smoothed using the *v.generalize* ('snakes' method, threshold: 20) tool within GRASS GIS. The "snakes" method retained the generalized shape of a line but removed sharp deflections in direction by minimizing the "energy" of the line (https://grass.osgeo.org/grass70/manuals/v.generalize.html; accessed 2015-09-01). The smoothing threshold was chosen by visually comparing the LIDAR-based channel networks at Millport Slough to channels mapped in the field by So *et al.* (2009).

Channel segments were organized into networks by tracing from the lowest segment with the highest Horton channel order in a network upstream to the highest using a recursive search algorithm that consumed the topological information provided by the *r.stream* family of tools. Segments were allowed to connect to multiple upstream segments and the network distance for each segment was calculated from the generalized channel segment lengths.

For more information regarding channel network extraction methods, please contact the authors of this report.

LIDAR-derived channel cross-sections

Perpendicular channel cross-sections were generated every 10 m along the entire length of each of the extracted tidal channel networks. Each cross-section extended 30 m perpendicular to the instantaneous direction of the flowpath at each cross-section station. Next, the LIDAR point cloud was extracted by extracting all LIDAR points within 1 m of either side of the cross-section. A one-dimensional DEM for each cross-section was created by applying a rolling minimum-bin filter with a 1 m window to assign elevations to location along the cross-section while mitigating vegetation interference in the DEM.

Bankfull width was extracted by fitting a quadratic function to the cross-section profile within 3 m of the flowpath. At every centimeter from the flowpath elevation to the highest elevation in the profile, the distance from the quadratic function to the profile was calculated. If this distance exceeded 6 m on either side of the flowpath, BFW was identified as the intersection with the profile at next-lowest elevation. Other methods (including fitting splines) were evaluated by ETG, but given significant noise in the data, the approach presented in this report performed the best. If BFW could not be extracted from the DEM, we excluded the cross-section from further analysis. Depth was calculated by subtracting the flowpath elevation from the BFW elevation. Finally, channel bank slope was calculated by calculating the mean of the slope of left top of bank to the flowpath and the slope of the right top of bank to the flowpath.

Unfortunately, as described in the **Introduction** above, the automated extraction of channel cross-sections from LIDAR did not produce usable data (primarily due to noise in the data), so the results are not presented in this report. Please contact the authors for more information.

Wallooskee-Youngs channel network extraction

We digitized the Wallooskee-Youngs channel network from USDA's National Agricultural Imagery Program (NAIP) 2014 imagery, for three reasons. First, water was impounded behind flow control structures of the restoration site, preventing adequate LIDAR imaging of the channel shape. Second, although we applied the automated channel extraction algorithm used for the reference sites, it did not perform well at this site; for example, it mapped remnant channels and flowpaths within the agricultural field that did not represent active channels at the site, based on our field experience. Finally, our automated channel extraction algorithm was calibrated against least-disturbed tidal wetlands, and therefore would not be expected to perform well in subsided and simplified channel networks within a disturbed site such as Wallooskee-Youngs. For these reasons, heads-up digitization from NAIP 2014 (1 m^2 spatial resolution) natural-color imagery was used to trace channels and ditches internal to the Wallooskee-Youngs restoration site. All channels and ditches were digitized at a consistent spatial scale of 1:1500 in ArcGIS (version 10.2.1, ESRI, http://esri.com). From this network, total channel network length, sinuosity, and density were calculated and compared with the reference sites.

Wallooskee-Youngs channel cross-section analysis

Field surveys of channel cross-sections were available for the Wallooskee-Youngs site and provided an appropriate source for calculating BFW, depth, and WTD. The Wallooskee-Youngs channel cross-section survey data were provided by Statewide Land Surveying Inc. in a geospatial point dataset coded with cross-section number, easting, northing, and elevation projected to the Oregon State Plane North horizontal coordinate system and referenced to the North American Vertical Datum (NAVD88) (Statewide Land Surveying Inc., 2012). To match the LIDAR data, the dataset was projected to Oregon Lambert (http://www.oregon.gov/odf/pages/gis/olamproj.aspx, accessed 9/30/2015) using ArcGIS (version 10.2.1, ESRI, http://esri.com).

We created line features for each cross-section in the GIS by connecting the first measurement (left bank) to the last measurement (right bank) in the point dataset. Point measurements along each cross-section were snapped to the line feature to remove small (< 30 cm) field deviations from a straight line. Next, the distance from the start of each cross-section to each measurement point along the cross-section was calculated. As described in the following sections, various metrics that describe the channels were calculated from the dataset and compared to reference channels. The flowpath distance for each cross section was calculated by tabulating the along-channel distance from the cross section to the channel mouth (junction of the channel network and the main river).

Reference site field-based channel cross-section survey

ETG surveyed channel morphology at the Daggett Point and Cooperage Slough reference sites to compare the LIDAR method to field measurements. We surveyed 11 cross-sectional transects at Daggett Point and eight transects at Cooperage Slough. Each transect spanned the tidal channel and included one general wetland surface measurement on each side of the channel. Transect locations were chosen in the field to capture representative channel morphology profiles in narrow (< 5 m BFW) channels and within different vegetation communities.

The start and end of each transect was measured and monumented with a temporary benchmark with high-precision RTK GPS equipment (Spectra Precision ProMark 220) to assign a horizontal position and elevation; positions were referenced to UTM Zone 10N and NAVD88. Next, we established a transect baseline using a CAM-Line thin-diameter graduated metal tape stretched between transect ends. We used a laser level to measure elevation at topographic breaks along the transect relative to the endpost monument. For each elevation measurement, we recorded the distance of that measurement along the transect and the associated feature (e.g., left bank, flowpath, right bank). Within the GIS, we calculated the horizontal position and reprojected the data to Oregon Lambert using ArcGIS to match the LIDAR and other data related to the Wallooskee-Youngs project.

A fully random or systematic sampling design with replication was not feasible nor the primary purpose of the measurements. Field-based sampling was also limited by logistical constraints and the difficulty of moving through the sites (the reason for our development of the LIDAR approach). Therefore, statistical comparisons of field-based channel cross-section to the reference site or among sites may not be appropriate. Therefore, we provide qualitative comparisons between field-based measurements at reference and restoration sites but do not make statistical inferences based on field measurements.

Derived metrics and comparisons of restoration *versus* reference sites

We calculated various channel network metrics to describe and compare channel structure and site channel characteristics at two spatial scales. These included total channel network length, number of outlets, channel density, per-channel length, per-channel gradient, and per-channel sinuosity.

Two spatial scales are represented by these metrics. The smallest-scale metrics (covering the largest area) are "site-level" metrics; these include total channel network length, number of outlets, and channel density. These metrics consider all channels in a given site (DP, FI, GI, or CS) as one element – without replication within a site. We also calculated additional metrics describing the characteristics of individual channels within a site (*i.e.*, "channel-level" metrics, including per-channel length, gradient, and sinuosity). These were calculated for all individual channels (from headwaters to mouth at the river or bay), and thus are replicated within a site. All replicates were then averaged to generate a mean for each metric. For example, per-channel length was the mean of many values, where each value was the length of a unique channel from initiation point to its network outlet. Multiple channels were evaluated statistically to derive a mean per-channel length for a given site.

Statistical analysis

All statistical analyses were performed in R (version 3.2.1). Normality in the data was tested using a Shapiro-Wilk test. Within this report, all of the channel morphology metrics analyzed were non-normal and could not be transformed into a normal distribution. Therefore, the non-parametric Kruskal-Wallis rank sum test was used to test significance. Statistical differences were considered significant if the p-value was less than 0.05, representing a 95% significance level. Post-hoc non-parametric Wilcoxon rank sum tests were used to test differences between sites.

Results and discussion

Channel networks and their associated metrics at the references sites were successfully extracted using the methods described above. Significant differences were found between the Wallooskee-Youngs site and the reference sites and among the references site; these differences are explained in the sections below.

Channel network length, number of outlets, and channel density

The Wallooskee-Youngs site had 7.54 km of channel and ditches within a total site area within the elevation range of the tides of 70.6 ha -- a channel density of 10.68 km/km^2 (Table 2, Figures 5-7). All channels and ditches exited the site through four outlets (Figures 5 and 8). Within the Wallooskee-Youngs site, channels had been reconfigured from their historical configurations to improve drainage. For example, the ditch that ran along the perimeter of the site at the base of the dike was excavated following the conversion to agriculture.

Ditches in the southern part of the Wallooskee-Youngs site were likely straightened or excavated to drain the site to the perimeter ditch and eventually exit the site through outlets in the northwest and southeastern sections of the site (Figure 5). The channels and ditches in the northern section of the site converge into a main channel that was likely excavated to better convey water out of the site through water structures (*e.g.,* tide gates) during low tides. Besides the channels mapped in Figure 5, other sinuous remnant channels were visible in the NAIP imagery and within the LIDAR data. However, most of these no longer regularly convey water through the site, although they may carry water during rainy periods.

Table 2. Total channel network length and density for each of the Youngs Bay estuary study sites. Channel network length was digitized from NAIP 2014 for the Wallooskee-Youngs restoration site and determined using LIDAR for the reference sites, as described in the methods section.

Site	**Site type**	**Site area (ha)***	**LIDAR-derived number of channel network outlets**	**Total channel network length (km)**	**Channel density (km / km^2)**
Wallooskee-Youngs (WY)	Restoration	70.64	4	7.54	10.68
Daggett Point (DP)	Reference	19.95	55	10.41	52.17
Fry Island (FI)	Reference	8.46	29	3.58	42.37
Grant Island (GI)	Reference	19.10	50	9.05	47.37
Cooperage Slough (CS)	Reference	52.37	10	27.37	52.27

*area below 4.3m, digitized from LiDAR

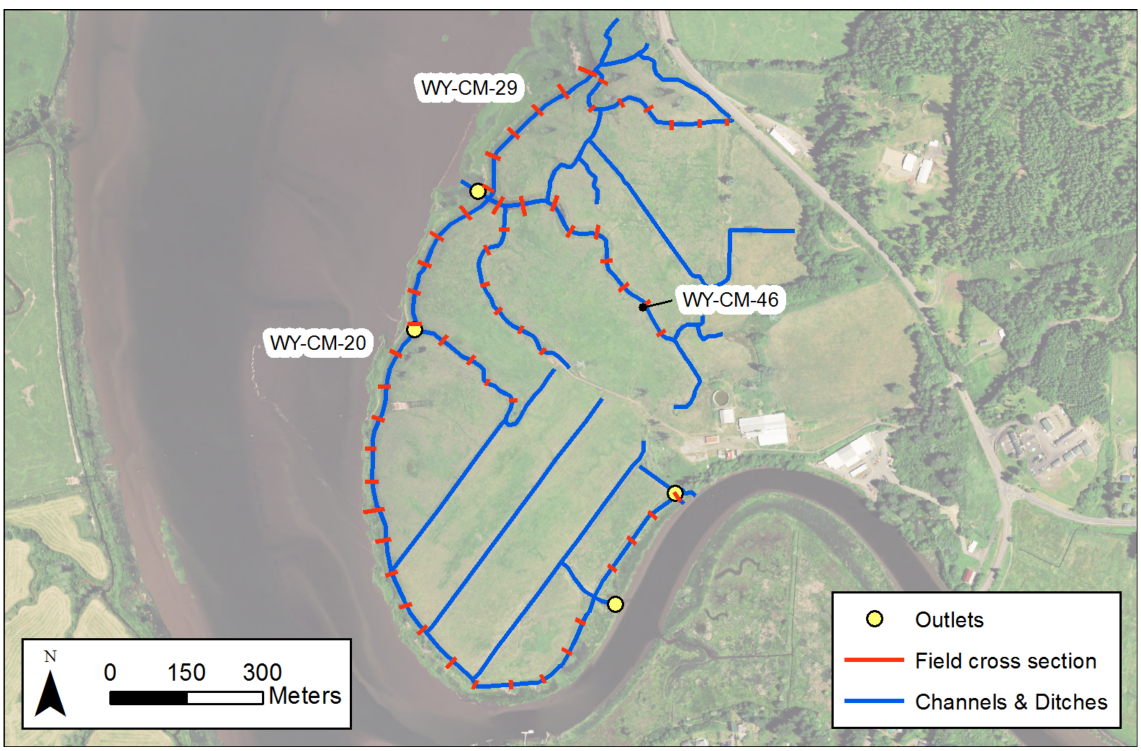

Figure 5. Channel and ditch network at the Wallooskee-Youngs restoration project, digitized from NAIP 2014 imagery. Red lines represent field-based channel morphology transects analyzed by ETG using data from Statewide Land Surveying Inc. (2012). Background: NAIP 2014.

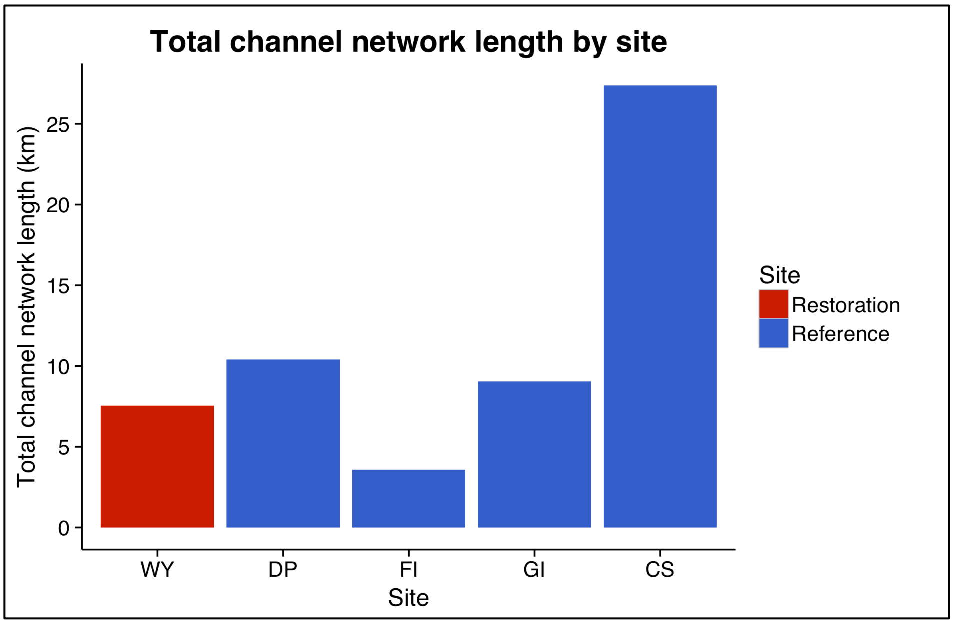

Figure 6. Total channel network length by site. Channels at the Wallooskee-Youngs restoration site were digitized from NAIP (2014) while the reference site channel networks were extracted from LIDAR.

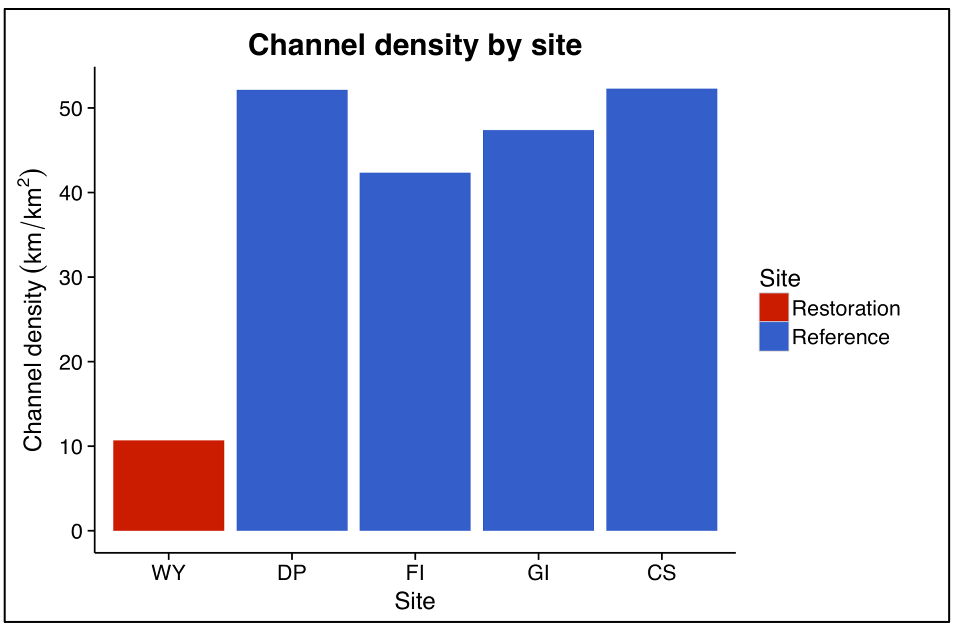

Figure 7. Channel density. Channel density represents the total length of a site's channel network divided by the area of the site. Channels at the Wallooskee-Youngs restoration site were digitized from NAIP (2014) while the reference site channel networks were extracted from LIDAR.

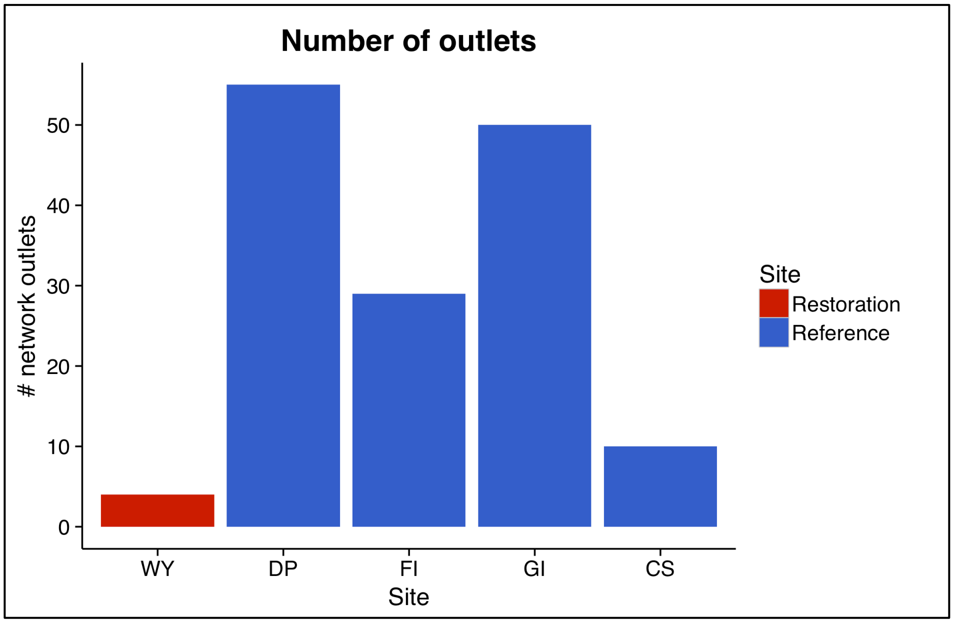

Figure 8. The number of channel network outlets to the main river channel or out of the sites. Channels at the Wallooskee-Youngs restoration site were digitized from NAIP (2014) while the reference site channel networks were extracted from LIDAR.

The channel networks at the least-disturbed reference sites differed dramatically from the Wallooskee-Youngs restoration site. At the Daggett Point reference site, channel network length totaled 10.41 km and channel density was 52.17 km/km^2, the second-highest density of all four reference sites (Table 2, Figures 6-7). These channel networks exited the site to the main river through 55 outlets (Table 2, Figure 8). Of these outlets, 50.9% exited the site with a Horton channel order equal to one, meaning that the channel initiated and immediately left the site without first connecting to another channel. Horton channel order was two at 27.3% (15) of the outlets at Daggett Point, and Horton channel order was three or four for the remaining 21.8% (12) of channel network outlets. At Daggett Point, the largest channels (Horton channel order 3 and 4) exited the site in the northeastern and southwestern quadrants (Figure 9). The large channel in the site's northeastern quadrant may have been excavated or straightened to support construction of the adjacent power transmission tower.

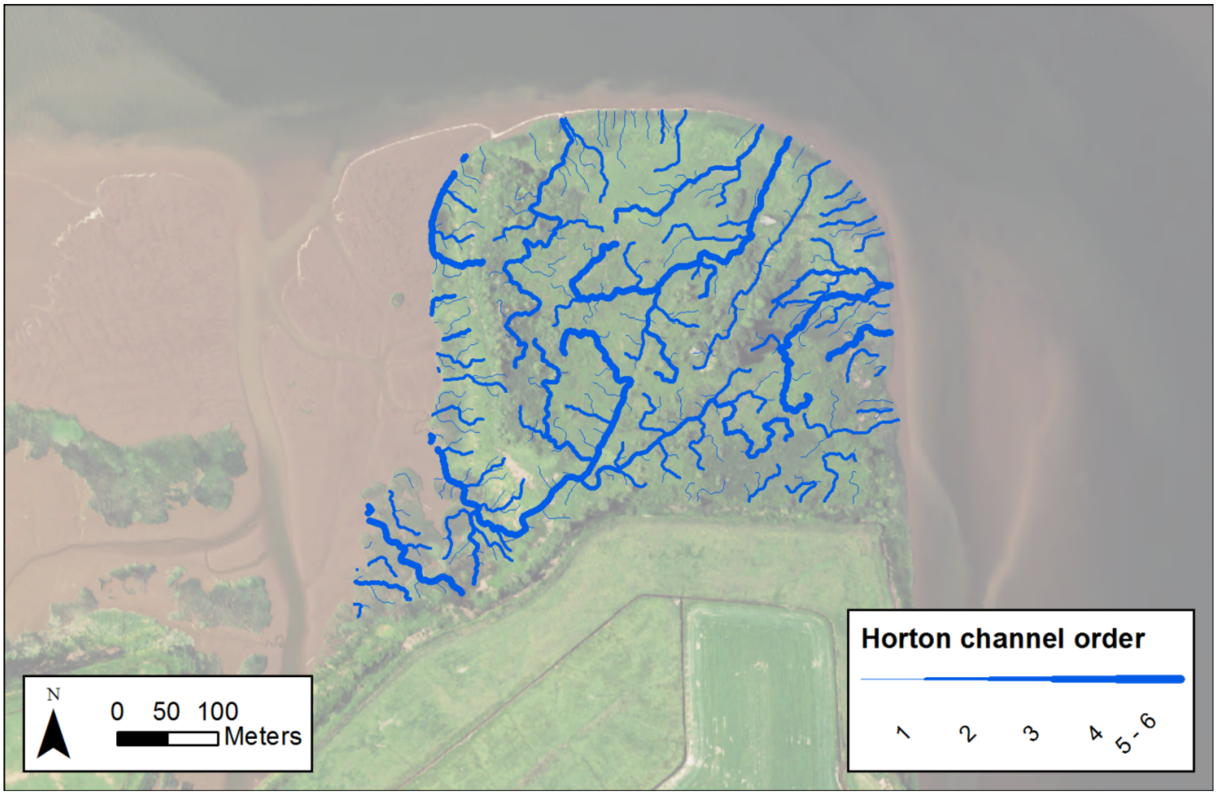

Figure 9. Daggett Point tidal channel network, extracted from LIDAR. Line widths represent Horton channel order. Background: NAIP 2014.

Fry Island was the smallest of the reference sites (8.46 ha) and had the shortest and least dense channel network of all four reference sites. Channel network length at Fry Island totaled 3.58 km and channel density was 42.37 km/km^2 (Table 2, Figures 6-7). Horton channel order was 1 or 2 for 75.9% (22) of the channel outlets at the site; the remaining 24% (7) of outlets were third channel order or higher. The largest channel (Horton channel order 5) exited the site to the West (Figure 10). Channels were oriented perpendicular to the flow of the Youngs River.

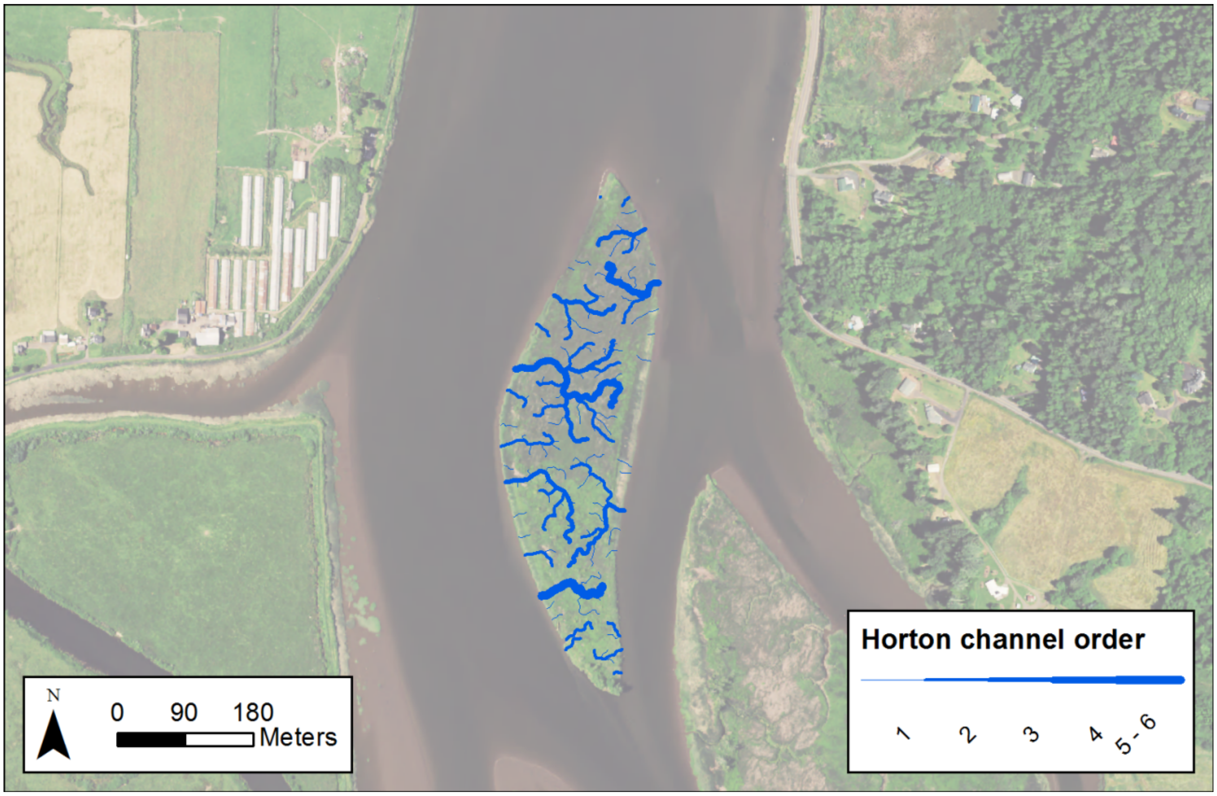

Figure 10. Fry Island tidal channel network extracted from LIDAR. Line widths represent Horton channel order. Background: NAIP 2014.

Immediately adjacent and upriver from Fry Island was Grant Island (Figure 11), with a total channel network length of 9.05 km and channel density of 47.37 km/km^2 (Table 2, Figures 6-7). Water within the Grant Island channel network exited the site through 50 outlets. Of these, 70% (35) exited as first- or second-order channels and 30% (15) exited as third- or fourth- order channels. Within the site, the largest channels exited the site to the east and west, perpendicular to the flow of the Youngs River. First-order channels exited the site around the perimeter of the site; these were generally short channels draining only the edge of the site.

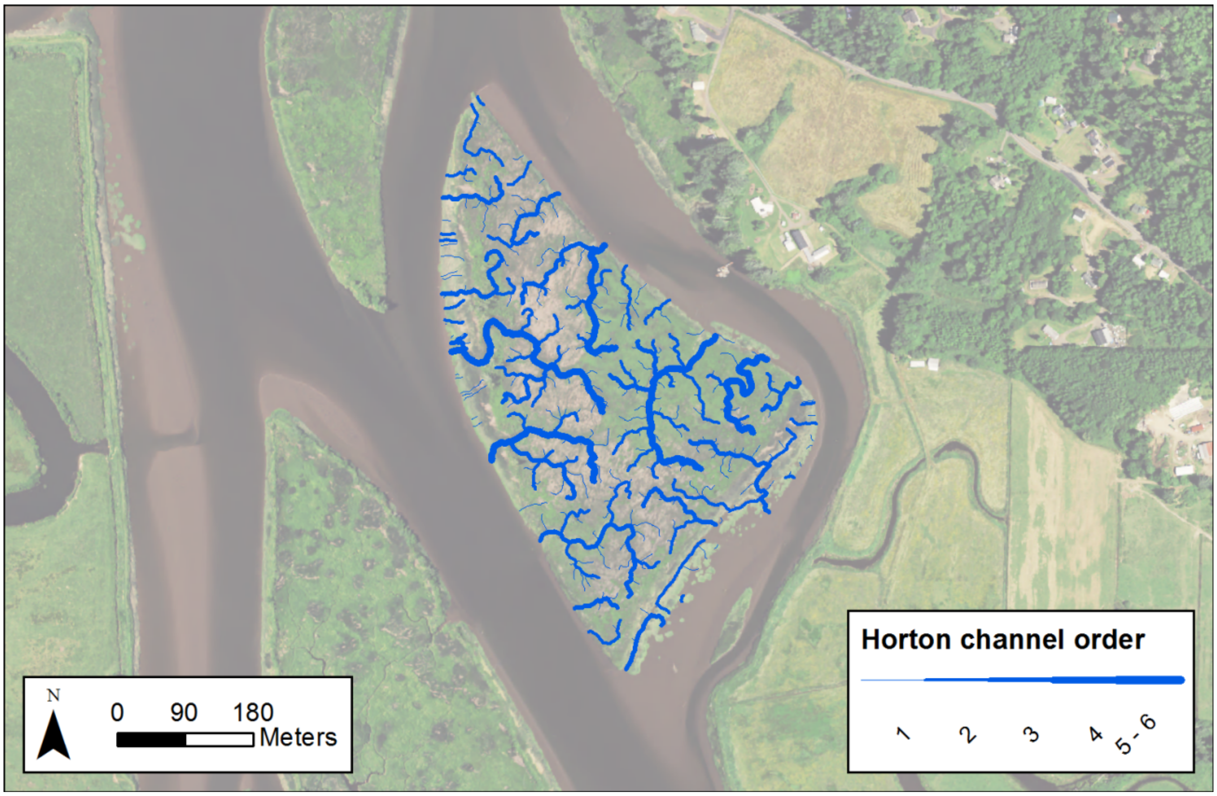

Figure 11. Grant Island tidal channel network extracted from LIDAR. Line widths represent Horton channel order. Background: NAIP 2014.

Finally, Cooperage Slough had a total channel length of 27.37 km and a channel density of 52.27 km/km^2 (Table 2, Figures 6-7). The channel network at Cooperage Slough had the longest total channel length and highest channel density of the reference sites (Figure 12). This site also had the fewest channel outlets (10) among the reference sites; the channel network was more dendritic and converged into two main channel outlets (Horton channel orders of 5 and 6). Of the site's 10 outlets, 30.0% (3) had a Horton channel order of one at the time of exit, while 40% (4) channel network outlets were second and third order. The largest channels (Horton channel order 4-6) represented 30% (3) of the outlets.

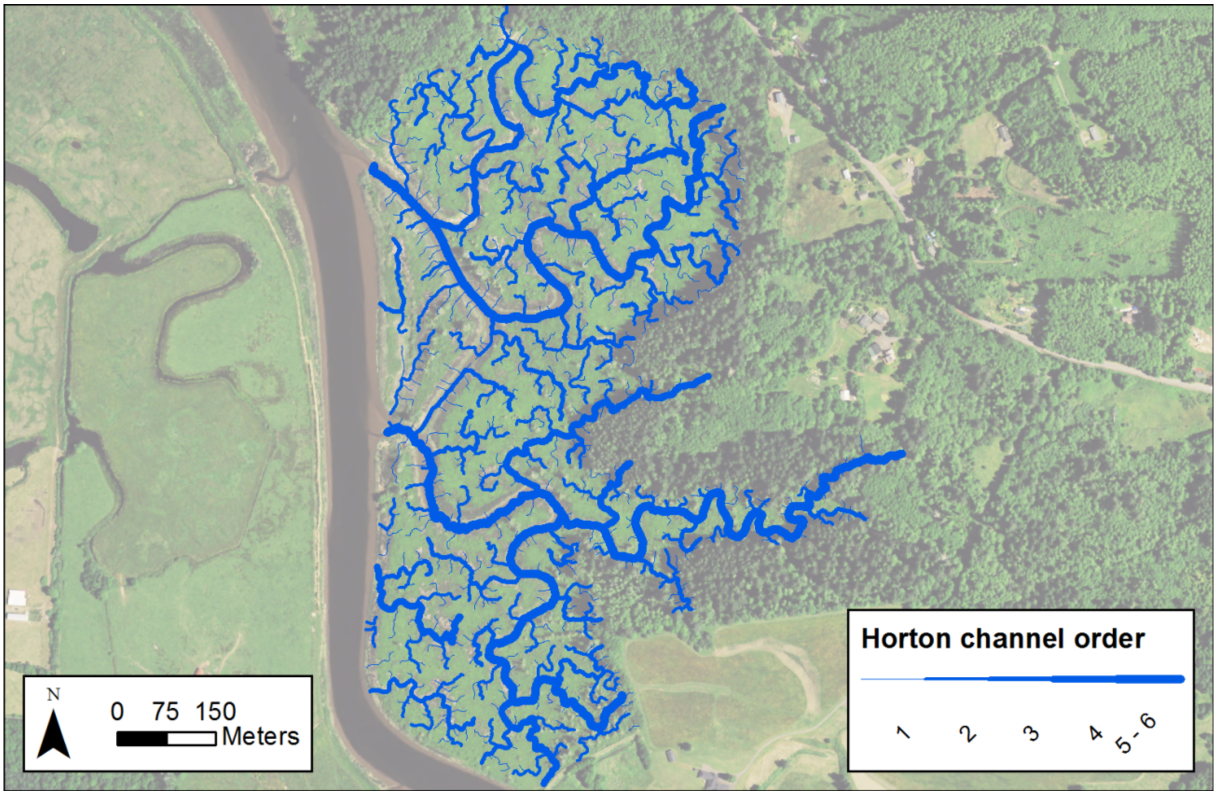

Figure 12. Cooperage Slough tidal channel network extracted from LIDAR. Line widths represent Horton channel order. Background: NAIP 2014.

Compared to the other reference sites, Cooperage Slough lacked the short, fringing first-order channels exiting directly to the river. This site is the furthest upstream and thus is most sheltered from wind-generated waves and weather in the bay, so wind-wave energy was likely lower at Cooperage Slough than at Daggett Point, Fry Island, or Grant Island. However, fluvial energy is likely strong at Cooperage Slough, due to its landscape setting on the floodplain of a relatively confined section of the Youngs River valley and less than 700 m downstream from the Youngs-Klaskanine confluence. Fluvially-dominated floodplain sites often have substantial natural levees resulting from river flooding during large precipitation events, which carry heavy loads of watershed-derived sediment. Natural levee formation on the western edge of Cooperage Slough, coupled with the lower level of wind-wave energy, may have contributed to the lower number of channel outlets from the site, and to the site's more dendritic and interconnected channel network.

Restoration-reference site comparison of channel density and outlet number

At the site level, the channel density metric provided the clearest illustration of the differences between the restoration site and reference marshes, because this metric is normalized to the size of the site.

Channel density at Wallooskee-Youngs was reduced by around 78% (range 75% to 80%) compared to the reference channel networks (Table 2, Figure 7). During conversion to agricultural uses, the smallest channels were likely filled, tilled or degraded through livestock trampling, while larger channels were likely enlarged or straightened to rapidly convey water out of the site. Overall channel length, and therefore density, within a site is greatly reduced when the smallest channels are removed or destroyed, since the great majority of total channel length is comprised of first and second order channels (So *et al*. 2009). We observed the same pattern at other restoration projects on the Oregon Coast. At the Waite Ranch restoration project in the Siuslaw River estuary, channel density was reduced by 89%, from around 69.65 km/km^2 to 7.95 km/km^2 (Brophy and Lemmer 2013, Figure 13). The reduction in channel density coupled with the straightening and rerouting of channels at Wallooskee-Youngs (Figure 5) compared to its reference sites (Figures 9-12) was visually similar to Waite Ranch in the Siuslaw River estuary (Figure 13).

Figure 13. Channel network density comparison for an unrestored, diked former tidal wetland and a least-disturbed tidal wetland. **Left:** simplified channel (ditch) network in a 30.35 ha section of Waite Ranch in the Siuslaw River estuary, Oregon. Channel density is 7.95 km/km^2; channel length is 1.61 km. **Right:** dense, dendritic channel network in a 30.35 ha section of least-disturbed high tidal marsh (Millport Slough, Siletz Bay NWR; black lines show a complete field survey of channels (So *et al*. 2009), most of which are not visible in aerial photos. Channel density is 59.65 km/km^2; channel length is about 17.71 km. Figure from Brophy and Lemmer (2013).

The number of channel network outlets from the Wallooskee-Youngs site to the Youngs River has also been reduced by conversion to agriculture, compared to the reference sites. Our data shows 86% to 92% fewer channel outlets at Wallooskee-Youngs compared to Fry Island or Grant Island, and 60% fewer outlets than Cooperage Slough. This reduction reflects active management; the number of outlets at a farmed site is generally managed to minimize maintenance of water control structures.

At Daggett Point, Fry Island, and Grant Island, our analysis identified more outlets than would be predicted based on relationships published for the Pacific Northwest. For example, Hood (2014) established a linear relationship between wetland area and the number of channel outlets for Youngs Bay and incorporated Daggett Point within his analysis. For a site the size of Daggett Point, Hood (2014) predicts nine outlets; by contrast, our LIDAR analysis identified 55 outlets (although many of these were short first-order channels draining only the wetland's edge). If channel networks that exit the site as first or second Horton order channels were ignored, the number of outlets (12) was closer to, but still exceeded Hood's predictions. The same pattern existed at Fry Island and Grant Island. For a site the size of Fry Island, Hood (2014) predicted five outlets, while our LIDAR-based method identified 29 outlets, of which only seven were third order or larger. Similarly, for a site the size of Grant Island, Hood (2014) predicted nine outlets, while our method identified 50 outlets. Of the outlets at Grant Island, 15 were third order or larger.

At Cooperage Slough, by contrast, our results were more similar to Hood's (2014) predictions. Our LIDAR analysis mapped 10 outlets; whereas Hood's (2014) analysis would predict 18 outlets.

The discrepancy between Hood's predictions and our analysis at Daggett Point, Grant Island and Fry Island may have been the result of methodological differences. First, Hood's method digitized channel networks from high-resolution aerial photography instead of using automated flow-routing algorithms on LIDAR (Hood 2007). As a result, channels could only be digitized where visible channels exist in the imagery. Small channels, such as the first and second order channels in our analysis, may have been obscured by vegetation and therefore difficult to delineate using aerial photo interpretation and heads-up digitization. Second, even though we calibrated our LIDAR analysis method using field data, our LIDAR method may have over-predicted the presence of small channels (low channel order) channels within a site. Over-prediction of channel presence would inflate total channel length, density, and network outlet estimates. However, the reference site channel densities we obtained from LIDAR analysis were similar to or slightly lower than the densities observed during a complete field survey of channels at Millport Slough in the Siletz River estuary (a similarly least-disturbed site), so we have confidence that LIDAR is not seriously over-predicting channels in this study. Additional fieldwork is recommended to verify the extent and topology of LIDAR-extracted channel networks, and to further explore the sources of discrepancies between our results and those of Hood (2014).

Relevance to restoration design

Based on the relationships Hood observed between site size and number of channel outlets, Hood (2014) suggested that restoration projects should include excavation of more channel outlets (i.e. more connections to the adjacent tidal water body). Although our LIDAR analysis indicated even more channel outlets than Hood predicted, we do not suggest that our results indicate a need for excavation of yet more channel outlets. Many of the outlets mapped using our LIDAR methods were small and drained only the edge of the wetland; they may also be shallow and very narrow. If they are in fact shallow, they would inundate only on the highest tides and would therefore be unlikely to contribute strongly to wetland functions such as fish habitat. Ground-truthing is needed to determine the proportion of the LIDAR-mapped outlets that are detectable in the field, and to determine the dimensions of those that are detectable. Restoration design recommendations could then be built using such data as a template for outlet design; the design should include site-specific adjustments to numbers and spatial configuration of outlets based on the landscape setting of individual restoration sites (since landscape setting appears to have a large effect on the number and positioning of channel outlets). Finally, natural processes are likely to create most of the small outlets mapped using our LIDAR methods, so excavation of these small outlets may actually be unnecessary.

Per-channel length, gradient, and sinuosity

LIDAR can also be used to analyze channel characteristics at a spatial scale less than an entire site. At this finer spatial scale, we used LIDAR to analyze per-channel length, gradient, and sinuosity. Each metric was calculated for every channel within a site from the point of that channel's initialization to its termination at the outlet to the main river. The data were then averaged across all individual channels within the network.

Per-channel length traces the distance from initialization to outlet for each channel within a site and is generally expected to be longer for larger sites. At the Wallooskee-Youngs restoration site, mean per-channel length was 545 meters; mean per-channel length was variable between reference sites (Table 3, Figure 14). Per-channel length at Wallooskee-Youngs was not statistically different from Cooperage Slough but was different from the remaining three reference sites (pairwise Wilcoxon Rank Sum Test, $p < 0.05$), as would be expected because those sites are smaller (Table 2). Differences among sites were likely primarily due to differences in site size. Daggett Point and Grant Island were nearly identical in wetland size and had a similar mean per-channel length. Daggett Point was 9.95 ha in size and had a mean per-channel length of 160 m while Grant Island was 19.10 ha and had a mean per-channel length of 126 m (Tables 2-3). Fry Island was the smallest (8.46 ha) and also had the shortest mean per-channel length of 81 m (Tables 2-3).

Table 3. Per-channel length, gradient, and sinuosity for each of the Youngs Bay estuary study sites.

Site	**Mean per-channel length, m (SE)**	**Mean per-channel gradient, % (SE)**	**Mean per-channel sinuosity (SE)**
Wallooskee-Youngs *	545 (64)	< 0.00 (< 0.00)	1.21 (0.04)
Daggett Point	160 (9)	1.37 (0.12)	1.45 (0.06)
Fry Island	81 (6)	4.64 (0.53)	1.37 (0.05)
Grant Island	126 (5)	1.76 (0.11)	1.50 (0.04)
Cooperage Slough	657 (14)	0.60 (0.03)	2.01 (0.03)
* Note: Values derived from digitized channel networks and field-based cross-sections instead of LIDAR.			

Per-channel gradient is the difference in elevation from initialization to outlet for each channel within a site, divided by that channel's per-channel length. The gradient was near zero for the restoration site, whereas reference site gradients ranged from 1% and 5% (Table 3, Figure 15). At Wallooskee-Youngs, channel gradients that approached zero may be evidence of excavation and alteration, as well as subsidence of the wetland surface. The gradient may have been reduced during channel dredging or ditch cleaning, or reduced due to sedimentation within the channel over time.

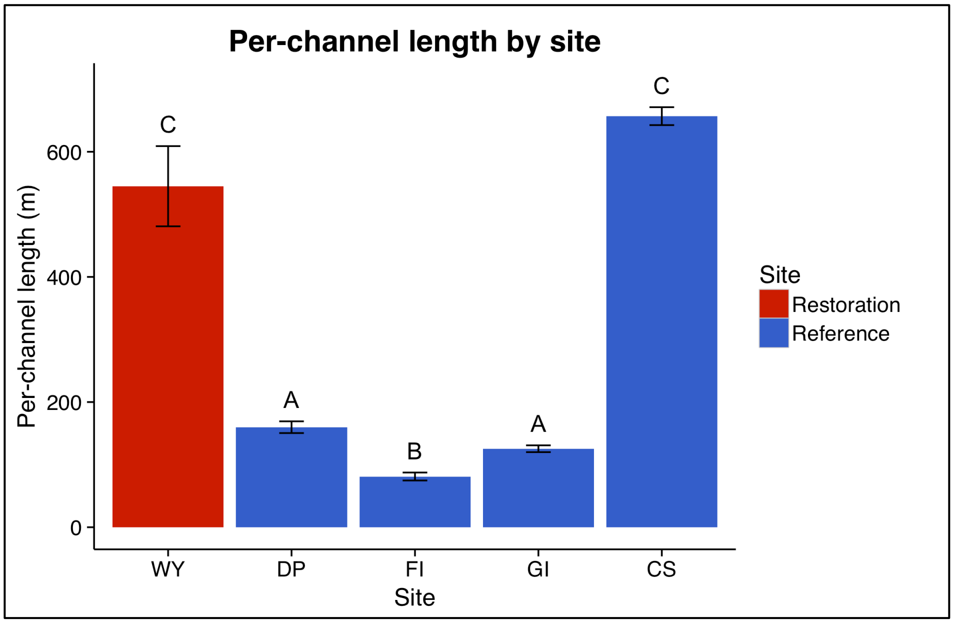

Figure 14. Mean LIDAR-derived per-channel length for each of the Youngs Bay estuary study sites. Bars with no letters in common were significantly different based on a pairwise Wilcoxon Rank Sum Test ($p < 0.05$). Error bars represent one standard error.

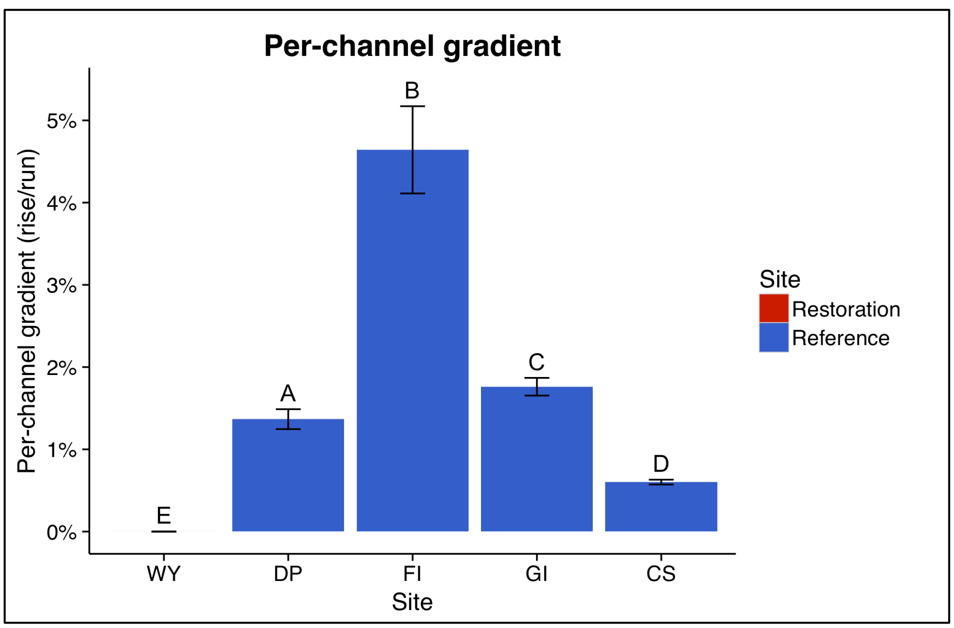

Figure 15. Mean LIDAR-derived per-channel gradient for each of the Youngs Bay estuary study sites. Mean per-channel gradient is calculated by dividing the total relief of a given channel by its along-channel length. Bars with no letters in common were significantly different based on a pairwise Wilcoxon Rank Sum Test ($p < 0.05$). Error bars represent one standard error.

Per-channel gradient at each of the reference sites was statistically different from the other reference sites (pairwise Wilcoxon Rank Sum Test, $p < 0.05$). Fry Island had the steepest per-channel gradient (4.64% grade) as channels were relatively short compared to the other reference sites, transitioning rapidly from initiation in the high marsh to their termination on the mudflat. Sites that were larger in size, such as Daggett Point and Cooperage Slough, had shallower channel gradients and longer channels (Table 3, Figure 14).

It is important to note that our measurements of per-channel gradient at the reference sites may be susceptible to vegetation interference with LIDAR that would artificially inflate the gradients. This interference could occur where vegetation obscures the LIDAR-derived elevation of the channel bottom at the point of initialization. However, the observed gradients seem appropriate given the geomorphic settings of the sites and in the context of the other data in this report. This potential bias did not apply to the Wallooskee-Youngs site, where channel gradients were derived from field survey data.

It is also important to note that channel gradients in least-disturbed sites are usually steepest in the upper reaches of each channel, with the longitudinal profile forming a "hook" shape with a relatively rapid rise to the wetland surface in the headwaters (Brophy *et al.* 2014, 2015). This information is important in designing channel systems for restoration sites.

Per-channel sinuosity describes the difference between the distance along a curving channel, divided by straight-line distance from channel initialization to outlet. Within the Wallooskee-Youngs restoration site, we expected per-channel sinuosity to be lower than the reference sites, due to channel straightening (ditching). Per-channel sinuosity at Wallooskee-Youngs was lower (1.21) compared to the reference sites (1.37 to 2.01) (Table 3); the difference was statistically significant for Wallooskee-Youngs compared to for Grant Island and Cooperage Slough (Figure 16). Grant Island had a channel sinuosity of 1.50 while Cooperage Slough had the most sinuous channels, with mean per-channel sinuosity of 2.01 (Figure 5). Daggett Point and Fry Island were not statistically different from each other and had mean per-channel sinuosities of 1.45 and 1.37 respectively.

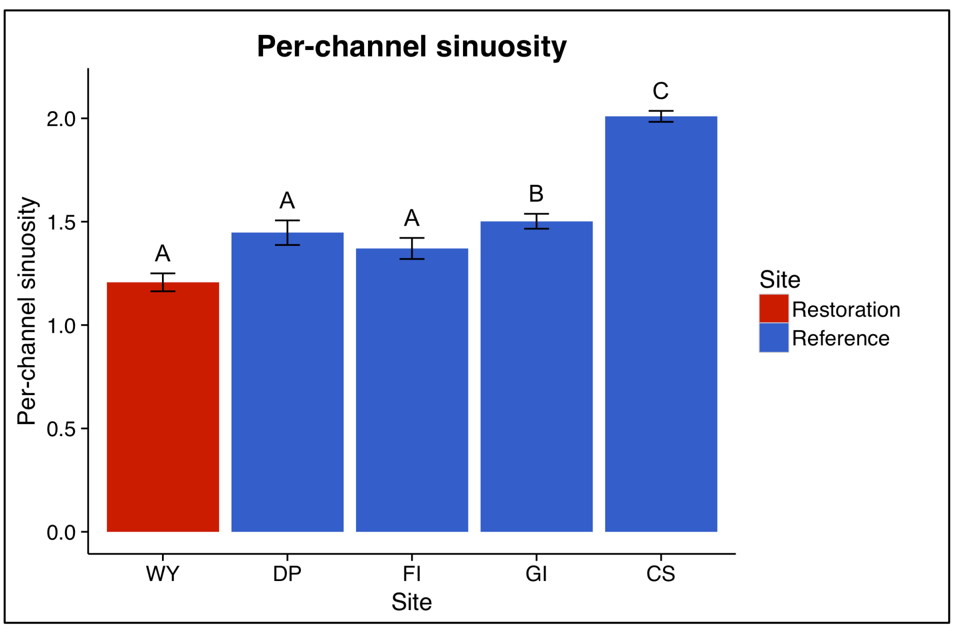

Figure 16. LIDAR-derived per-channel sinuosity for each of the Youngs Bay estuary study sites. Bars with no letters in common were significantly different based on a pairwise Wilcoxon Rank Sum Test ($p < 0.05$). Error bars represent one standard error.

Considering the prevalence of straight ditches at the Wallooskee-Youngs site, per-channel sinuosity was surprisingly high. However, the perimeter ditch that follows the western edge of the site inflates our sinuosity estimate at this site. This perimeter ditch collects many of the channels and ditches interior to the site (Figure 5). As a result, sinuosity measurements for each of these channels included the perimeter ditch, which inflated the along-channel distance while shortening the straight-line distance for each channel, increasing sinuosity. If sinuosity at Wallooskee-Youngs were calculated excluding the perimeter ditch, it would likely be much lower. Additionally, some of Wallooskee-Young's largest channels were remnant channels with relatively high sinuosity (northern half of the site, Figure 5). Finally, there were fewer channels at the Wallooskee-Youngs site compared to the reference sites. Therefore, the mean we derived from the data was more sensitive to abnormally long channels (like the perimeter ditch and remnant channel on the north half), compared to the reference sites. At the Waite Ranch restoration project in the Siuslaw River estuary, sinuosity for channels within the restoration site was near 1.0, compared to 1.5 to 2.0 for its reference channel network in the Siletz Bay site (So *et al*. 2009, Brophy *et al.* 2015).

Channel cross sections and flowpath elevation

ETG evaluated bankfull width, depth, flowpath elevation, and width-to-depth (WTD) ratio at the Wallooskee-Youngs restoration site using data from Statewide Land Surveying Inc. (2012). The purpose of this analysis was to document existing conditions at the Wallooskee-Youngs site prior to restoration, providing a baseline for evaluation of the trajectory of channel development after restoration.

Although ETG also conducted field measurements of reference site channel cross-sections, statistical comparison of restoration *versus* reference cross-section metrics is not recommended, and caution should be used when making these comparisons, because of different sampling methodologies and limited replication within size classes for each site. Therefore, we present statistical comparisons between channels within the Wallooskee-Youngs site, but make only descriptive comparisons to the reference sites. To better reflect existing data collected by others, we included channel profile data from Borde *et al.* (2011) in our comparisons between Wallooskee-Youngs and the reference sites.

Channels at the Wallooskee-Youngs restoration site were sorted into three BFW classes based on the Jenks natural breaks algorithm. Channels with a BFW of between 1.6 m to 7.0 m were represented by 23 transects at Wallooskee-Youngs. Channels with BFW between 7.0 m to 11.5 m were represented by 20 transects, while the largest channels of (BFW between 11.5 m and 21.1 m) were represented by eight transects (Figure 17, Table 4).

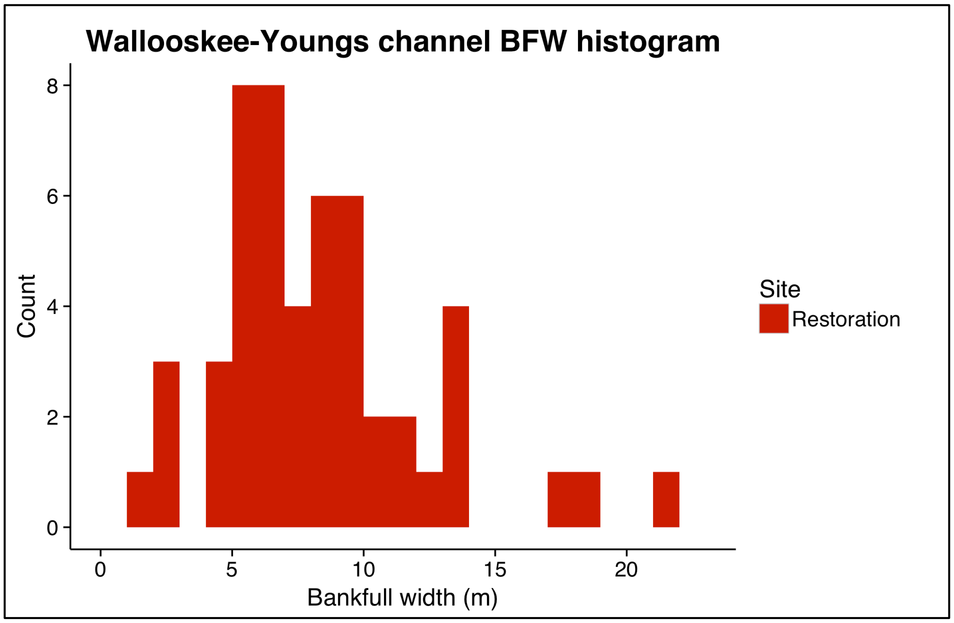

Figure 17. Bankfull width histogram (binwidth = 1 m) for the Wallooskee-Youngs restoration site.

Table 4. Wallooskee-Youngs channel cross-section characteristics (from data provided by Statewide Land Surveying Inc.), by width class.

BFW Class, m	Number of transects	Mean BFW, m (SE)	Mean depth, m (SE)	Mean WTD (SE)	Mean flowpath elevation, m (SE)
[1.6, 7.0]	23	5.0 (0.3)	0.98 (0.10)	6.1 (0.5)	0.53 (0.13)
(7.0, 11.5]	20	9.1 (0.3)	1.21 (0.09)	8.7 (1.0)	0.20 (0.04)
(11.5, 21.1)	8	15.7 (1.1)	1.10 (0.09)	14.8 (1.3)	0.24 (0.02)

Channel depths at Wallooskee-Youngs did not differ significantly between channel size classes (Figure 18). Mean depth across all channels at the restoration site was 1.09 m (SE: 0.01 m, n: 51). Channels between 1.6 m and 11.5 m wide had depths similar to channels in that width class at the reference sites (based on data from ETG fieldwork and Borde *et al.* 2011) (Tables 5-6). However, the widest channels (between 11.5 m and 21.1 m BFW) were shallower at Wallooskee-Youngs (1.1 m) compared to the reference sites (2.27 m) (Tables 4-5).

Table 5. Reference site channel cross-section characteristics from ETG field measurements, by width class. (Note: methods differed between the restoration (*i.e.*, Table 4) and reference sites, and data do not represent a random sample across all channels. Therefore, caution should be used when comparing data between the reference and restoration sites.)

BFW Class, m	Number of transects	Mean BFW, m (SE)	Mean depth, m (SE)	Mean WTD (SE)	Mean flowpath elevation, m (SE)
[1.6, 7.0]	24	1.8 (0.1)	0.67 (0.01)	2.8 (0.1)	1.46 (0.02)
(7.0, 11.5]	2	9.9 (0.5)	1.51 (0.01)	1.5 (0.3)	0.74 (0.09)
(11.5, 21.1)	2	16.7 (1.9)	2.27 (0.43)	8.3(2.5)	-0.25 (0.05)

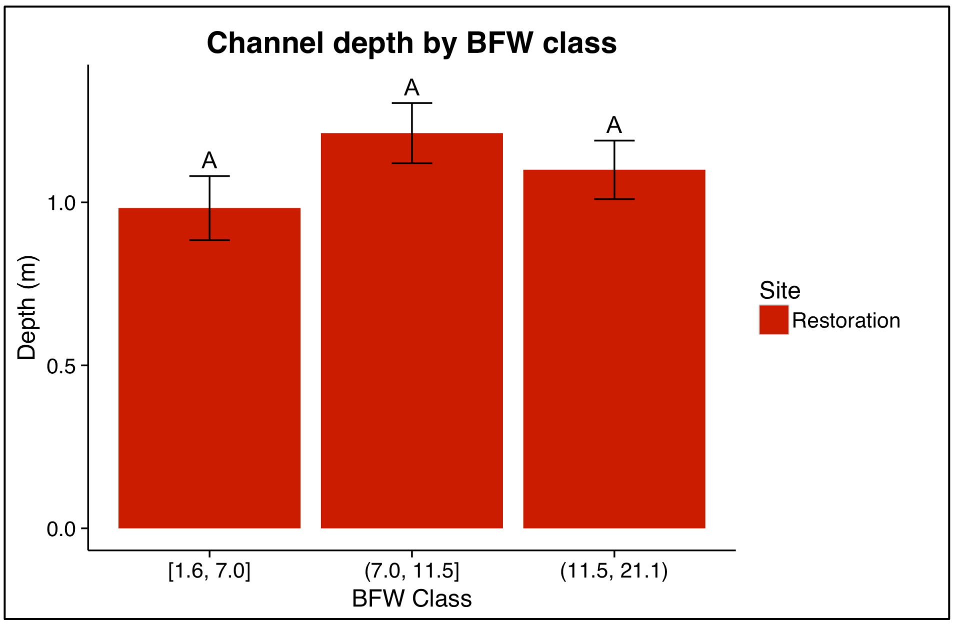

Figure 18. Channel depth by BFW size class within the Wallooskee-Youngs restoration site. Bars with no letters in common were significantly different based on a pairwise Wilcoxon Rank Sum Test ($p < 0.05$). Error bars represent one standard error.

Width-to-depth (WTD) ratios at Wallooskee-Youngs were similar for small and medium channels (BFW between 1.6 and 11.5 m), but the largest channels had significantly greater WTD ratios (Figure 19). Overall, WTD ratios were much higher at Wallooskee-Youngs compared to the reference sites (Tables 4 and 5), generally about twice as high as at the reference sites (using reference site data from ETG field measurements and Borde *et al*. 2011). Although the reference site data contained few examples of large channels, the trend was consistent across all channel width classes.

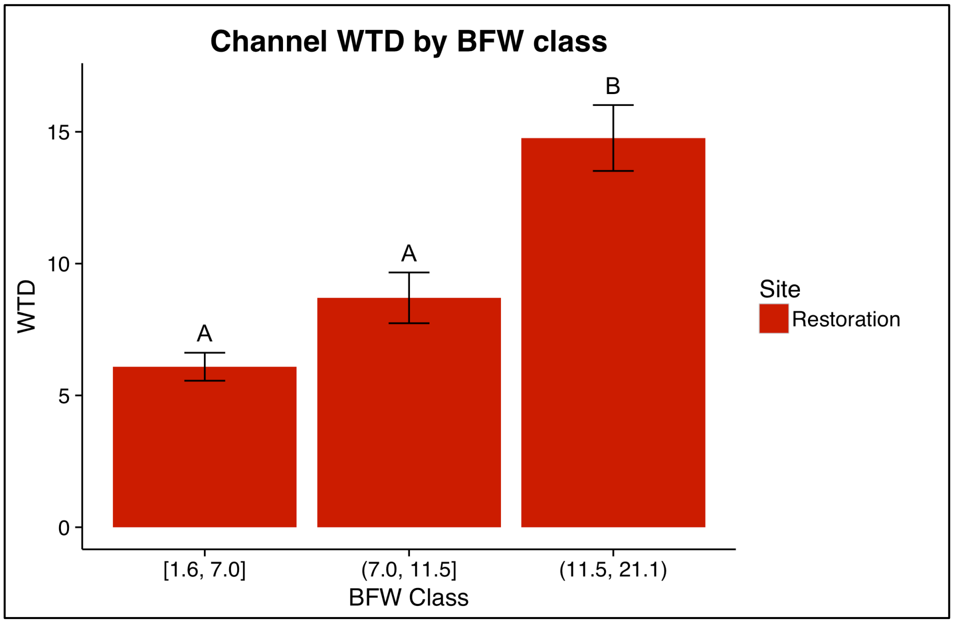

Figure 19. Channel width-to-depth (WTD) ratio by BFW size class within the Wallooskee-Youngs restoration site. Bars with no letters in common were significantly different based on a pairwise Wilcoxon Rank Sum Test ($p < 0.05$). Error bars represent one standard error.

Channel flowpath elevation (i.e., thalweg elevation) is the lowest elevation within a channel cross-section or transect. At the Wallooskee-Youngs site, flowpath elevation did not differ significantly among BFW classes, ranging from -0.2 m to 1.98 m NAVD88 (Figure 20). The smallest channels at Wallooskee-Youngs were the highest in elevation, yet the lack of statistical separation among groups indicates that the flowpath elevation was largely unrelated to channel size. This agrees with our observation of a channel gradient near zero at Wallooskee-Youngs (Table 3, Figure 14). Although individual channels differed in their flowpath elevations, they lacked a gradient that would result in detectable relationships between channel size and elevation.

For the reference sites, data from our fieldwork and Borde *et al.* (2011) showed a mean flowpath elevation of 1.46 m (SE: 0.02 m, n=24) for channels with a BFW between 1.6 m and 7.0 m (Table 5). Two transects at Grant Island measured by Borde *et al.* (2011) were between 7.0 m and 11.5 m BFW and had a mean flowpath elevation of 0.74 m (SE: 0.09, n=2). Finally, the largest channels at the site had a mean flowpath elevation of -0.25 m NAVD88 (SE: 0.05, n=2).

Comparing the data between Wallooskee-Youngs and reference sites, channels at Wallooskee-Youngs may have been excavated, but their flowpath elevations are still relatively high compared to reference channels, and also relatively high compared to restoration site channels in our previous studies. At Waite Ranch, an unrestored diked pasture in the Siuslaw River estuary, ditches had been excavated about 1.75 m deeper than reference site channels, especially towards the lower reaches of the channel network and in the largest channels (Brophy *et al*. 2015). Waite Ranch was heavily subsided, so most likely ditches had to be excavated to a great depth to successfully drain the site. At Wallooskee-Youngs, the ditch and channel network may have been effective at draining the site with less excavation of ditches and remnant channels.

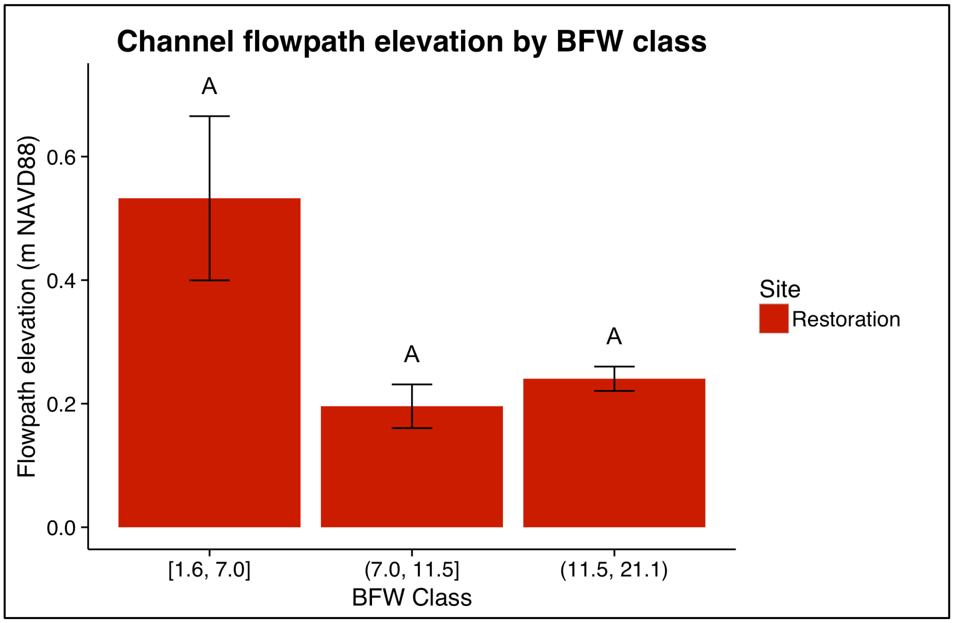

Figure 20. Channel flowpath elevation by BFW size class within the Wallooskee-Youngs restoration site. Bars with no letters in common were significantly different based on a pairwise Wilcoxon Rank Sum Test ($p < 0.05$). Error bars represent one standard error.

Graphs of channel cross-sections at Wallooskee-Youngs clearly showed the effect of alterations for agricultural use. Figures 17-19 show representative channel cross-sections for each bankfull width class at the Wallooskee-Youngs site. Transect locations are annotated on Figure 5.

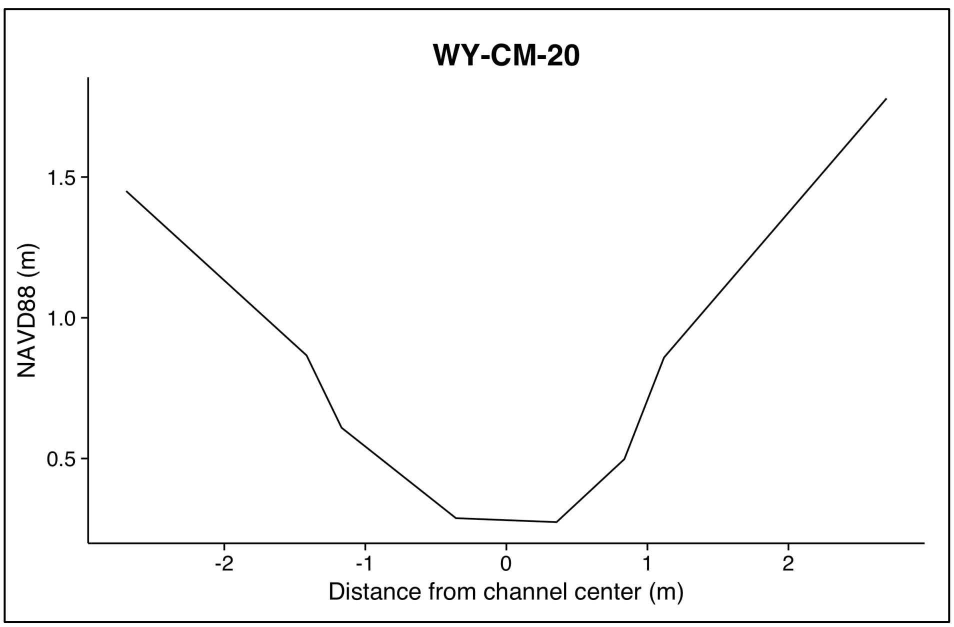

Figure 21. Channel cross-section from the Wallooskee-Youngs site with a BFW of 5.4 m, depth of 1.3 m, WTD of 4.0, and flowpath elevation of 0.27 m NAVD88. The profile is plotted with a 2:1 aspect.

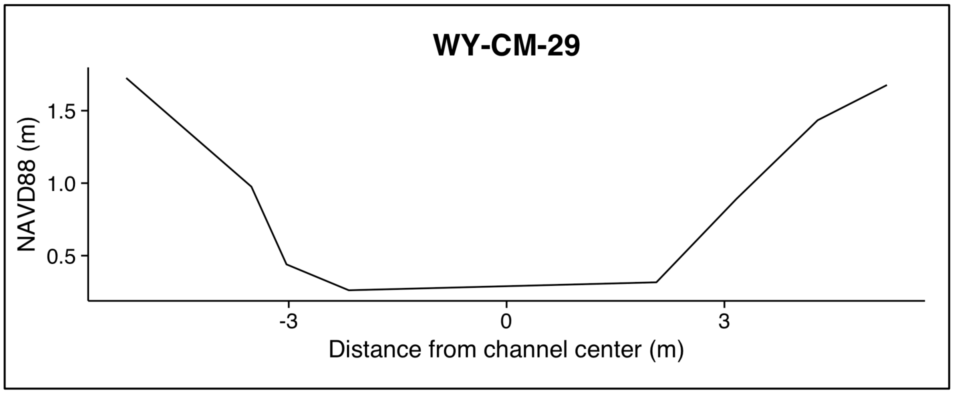

Figure 22. Channel cross-section from the Wallooskee-Youngs site with a BFW of 10.5 m, depth of 1.4 m, WTD of 7.3, and flowpath elevation of 0.26 m NAVD88. The profile is plotted with a 2:1 aspect.

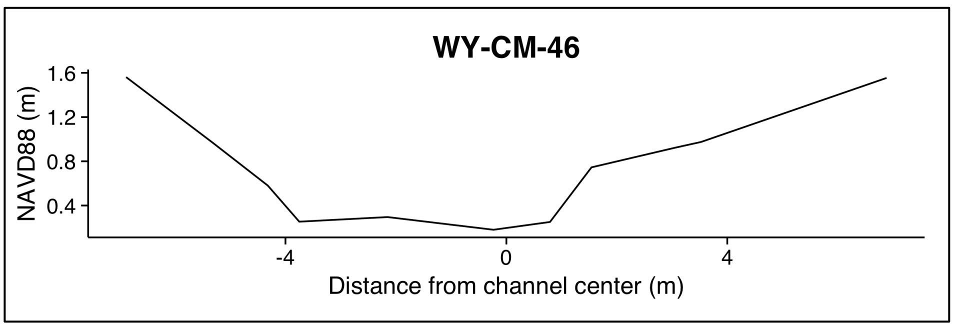

Figure 23. Channel cross-section from the Wallooskee-Youngs site with a BFW of 13.8 m, depth of 1.4 m, WTD of 10.0, and flowpath elevation of 0.18 m NAVD88. The profile is plotted with a 2:1 aspect.

Representative channels profiles from Borde *et al.* (2011) for Grant Island (Figure 24) and Cooperage Slough (Figure 25) had lower WTD ratios, indicating that the channels are narrower and/or deeper than the Wallooskee-Youngs restoration site. Each of the profiles had a sharp “V” shape with a clear flowpath at the lowest point of the cross section (Figures 24 and 25). In addition, the channel cross sections from the reference sites showed very steep channel banks, compared to the Wallooskee-Youngs channel cross sections. Steep channel banks – often near vertical – are common in small channels in least-disturbed tidal wetlands in the Pacific Northwest; due to dense, overhanging vegetation, these channels may be nearly undetectable from above, even when traveling on foot.

By contrast, the profiles from Wallooskee-Youngs showed a very flat channel bottom and overall trapezoidal shape. This channel shape is common in restoration sites, and likely results from a combination of sedimentation, livestock trampling, excavation, and low flow velocities over years of agricultural use. At Waite Ranch we observed the same pattern and attributed the shallower bank slopes at the restoration site to livestock trampling, subsidence of the site, and loss of organic matter and soil structure (Brophy *et al*. 2015).

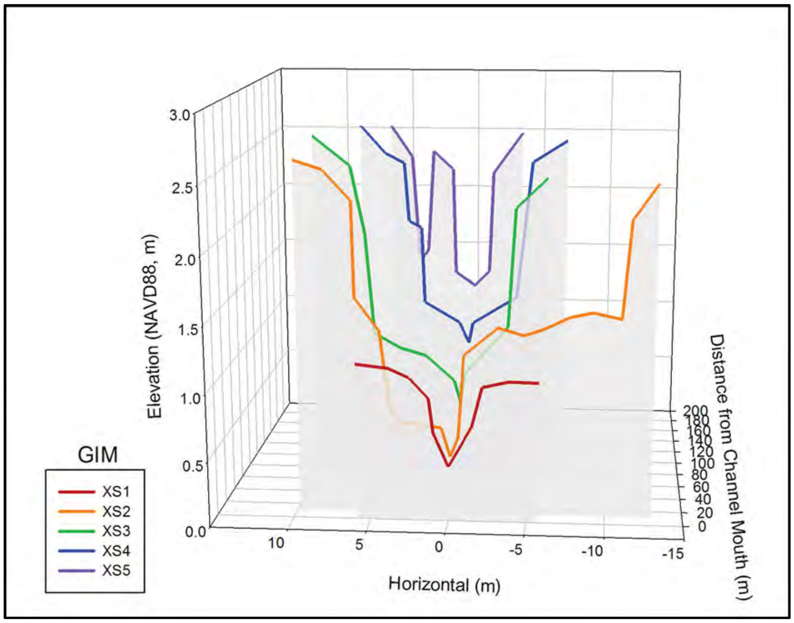

Figure 24. (**from Borde *et al.* 2011):** Five channel cross sections along the same channel at Grant Island with a BFW ranging between 3.0 m and 10.6 m, depth between 0.51 m and 1.53 m, WTD ratio between 3.1 and 6.9, and flowpath elevation between 0.41 m NAVD88 and 1.20 m NAVD88. The profiles are plotted with a variable aspect of about 20:1.

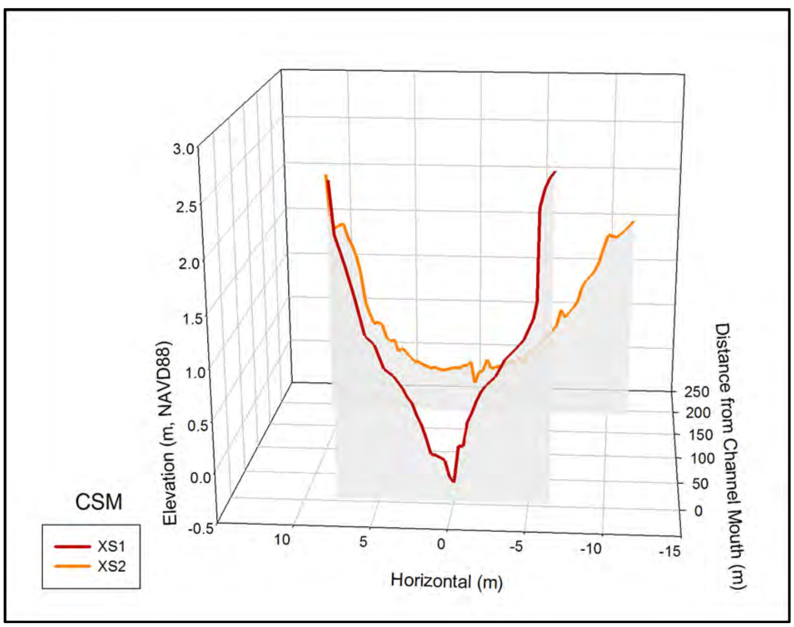

Figure 25. (**from Borde *et al.* 2011):** Two channel cross sections along the same channel at Cooperage Slough with BFWs of 13.9 m and 19.4 m, depths of 2.88 m and 1.65 m, WTD ratios of 4.8 and 11.7, and flowpath elevations of -0.31 m NAVD88 and -0.18 m NAVD88. The profiles are plotted with a variable aspect of about 20:1.

Summary

We present a new method to extract channel networks from LIDAR at four least-disturbed tidal wetlands in the Youngs Bay estuary, Oregon. The LIDAR-based method was calibrated against field data and used a least-cost approach to mitigate the effect of noise or small hummocks in the digital terrain model. From the LIDAR-derived channel network, we calculated a variety of channel morphology metrics at the site scale, including channel network length, number of outlets, and channel density. Within each site, metrics at the scale of the individual channel were also calculated, including per-channel flowpath length, gradient, and sinuosity.

At Wallooskee-Youngs, our results fit with expectations for a site that has been diked, ditched, and disconnected from tidal flow. Channel density at Wallooskee-Youngs has been reduced by around 78% (range 75% to 80%) compared to the reference sites. Channels at Wallooskee-Youngs had a reduced depth relative to top of bank and shallower bank slopes, and therefore greater width-to-depth ratios. The higher flowpath elevations at Wallooskee-Youngs compared to the reference sites indicated likely accumulated sediment. Agricultural use and ditching at Wallooskee-Youngs have greatly decreased overall channel length, density, and sinuosity.

Channel density ranged from 42.4 km/km^2 to 52.3 km/km^2 for the reference sites, with the highest channel density at Cooperage Slough and the lowest at Fry Island. Channel network length, number of outlets, and gradient varied among the least-disturbed reference sites and appeared to be related to the size of the wetlands and relative energetics of the sites. Our analysis identified more channel outlets to the main river then past studies for three of the four reference sites; many of the outlets were first-order channels that may have been previously overlooked and drain only the margins of the wetlands.

The LIDAR methods used in this study represent a potentially powerful tool for analyzing channel network characteristics. The results can be used to directly assess least-disturbed reference site functions such as fish habitat, and to relate least-disturbed channel conditions to other wetland functions. By comparing restoration site channel networks to these reference conditions, we can quantify of the impacts of site alterations on those functions. Finally, the reference site data provide a benchmark for tracking the post-restoration recovery of channel networks at restoration sites. To make best use of the LIDAR methods, we recommend field validation of the LIDAR-derived channel networks at representative sites.

Conclusions

At the Wallooskee-Youngs restoration site, channel characteristics reflect the elimination of natural processes and highlight the deliberate alterations made to allow economic use of the site. Shorter, straighter, and shallower channels dominated the restoration site, compared to the deeper, narrower, and more sinuous channels found at the reference sites. Channels transport tidewaters efficiently deep into a site, carrying nutrients that sustain food webs, creating fish habitat, and carrying sediments whose accretion allows tidal wetland elevations to keep pace with relative sea-level rise. The dynamic water level and salinity changes associated with dense, dendritic tidal channel networks also influence groundwater levels and groundwater salinity. Groundwater level and groundwater salinity are likely controlling factors for carbon cycling. For example, low salinities and constant saturation have been shown to increase release of methane (a greenhouse gas).

In summary, the channel network characteristics we observed in the least disturbed tidal systems are structural indicators of highly functional wetlands. These channel networks are the result of controlling factors such as tidal inundation regime, and in turn, channel networks mediate the effects of those controlling factors on other tidal wetland structures and processes, such as groundwater fluctuations, sediment accretion, and soil characteristics. These interlinked processes produce the valued ecosystem services provided by tidal wetlands, such as carbon sequestration, fish and wildlife habitat, nutrient processing, and flood mitigation. After restoration of the Wallooskee-Youngs site, we expect to see gradual recovery of the channel systems, leading in turn to recovery of the functions that depend on them.

During late 2015 through 2016, we will continue to analyze the carbon cores and monitor likely carbon sequestration drivers at the reference sites with funding from USFWS. These results will allow us to relate carbon sequestration to these drivers and to the channel systems we observed and mapped. We will report on results from that larger study at the end of 2016.

Literature cited

Athearn, N.D., J.Y. Takekawa, B. Jaffe, B.J. Hattenbach, A.C. Foxgrover. 2010. Mapping elevations of tidal wetland restoration sites in San Francisco Bay: Comparing accuracy of aerial LIDAR with a singlebeam echosounder. *Journal of Coastal Research* 262 (2): 312–19. doi:10.2112/08-1076.1.

Bater, C.W., and N.C. Coops. 2009. Evaluating error associated with Lidar-derived DEM interpolation. *Computers & Geosciences* 35 (2): 289–300. doi:10.1016/j.cageo.2008.09.001.

Brophy, L.S., S. van de Wetering, M.J. Ewald, L.A. Brown, and C.N. Janousek. 2014. Ni-les'tun tidal wetland restoration effectiveness monitoring: Year 2 post-restoration (2013). Corvallis, Oregon: Institute for Applied Ecology. Accessed 5/10/15 at https://www.dropbox.com/s/0g32kmqmmyjruf6/Nilestun_Year2_EM_report_FINAL_20140730-2.pdf?dl=0.

Brophy, L.S., L.A. Brown, and M.J. Ewald. 2015. Waite Ranch baseline effectiveness monitoring: 2014. Corvallis, Oregon: Institute for Applied Ecology.

Brophy, L.S., and J. Lemmer. 2013. Waite Ranch interim management plan. Prepared for Oregon Watershed Enhancement Board. Green Point Consulting, Corvallis, OR, and McKenzie River Trust, Eugene, OR. 56 pp.

Borde, A.B., Zimmerman, S.A., Kaufmann, R.M., Diefenderfer, H.L., Sather, N.K., and R.M. Thom. 2011. Lower Columbia River and Estuary restoration reference site study: 2010 final report and site summaries. PNNL-4262, Pacific Northwest National Laboratory, Richland, Washington.

Chassereau, J.E., J.M. Bell, and R. Torres. 2011. A comparison of GPS and LIDAR salt marsh DEMs. *Earth Surface Processes and Landforms* 36 (13): 1770–75. doi:10.1002/esp.2199.

Crooks, S., J. Rybczyk, K. O'Connell, D.L. Devier, K. Poppe, and S. Emmett-Mattox. 2014. Coastal Blue Carbon Opportunity Assessment for the Snohomish Estuary: The Climate Benefits of Estuary Restoration. Report by Environmental Science Associates, Western Washington University, EarthCorps, and Restore America's Estuaries. February 2014.

Diefenderfer, H.L., A.M. Coleman, A.B. Borde, and I.A. Sinks. 2008. Hydraulic geometry and microtopography of tidal freshwater forested wetlands and implications for restoration, Columbia River, U.S.A *International Journal of Ecohydrology & Hydrobiology* 8(2-4):339-361. doi:10.2478/v10104-009-0027-7.

Ewald, M.J., and L.S. Brophy. 2012. Tidal wetland prioritization for the Tillamook Bay Estuary. Prepared for the Tillamook Estuaries Partnership, Garibaldi, Oregon. Green Point Consulting, Corvallis, Oregon.

Ewald, M.J. 2013. Where's the ground surface? Elevation bias in LIDAR-derived digital elevation models due to dense vegetation in Oregon tidal marshes. Master's thesis, Oregon State University. Accessed 3/12/14 at http://hdl.handle.net/1957/45127.

Hawes, S.M., J.A. Hiebler, E.M. Nielsen, C.W. Alton, J. A. Christy and P. Benner. 2008. Historical vegetation of the Pacific Coast, Oregon, 1855-1910. ArcMap shapefile, Version 2008_03. Oregon Natural Heritage Information Center, Oregon State University. Accessed 5/31/12 at http://www.pdx.edu/sites/www.pdx.edu.pnwlamp/files/glo_coast_2008_03.zip.

Heiri, O., A. F. Lotter and G. Lemcke. 2001. Loss on ignition as a method for estimating organic and carbonate content in sediments: reproducibility and comparability of results. *Journal of paleolimnology*, *25*(1): 101-110.

Hladik, C., and M. Alber. 2012. Accuracy assessment and correction of a LIDAR-derived salt marsh digital elevation model. *Remote Sensing of Environment* 121 (2012): 224–35. doi:10.1016/j.rse.2012.01.018.

Hood, W.G. 2002. Application of landscape allometry to restoration of tidal channels. *Restoration Ecology* 10(2): 213–222.

Hood, W.G. 2004. Indirect environmental effects of dikes on estuarine tidal channels: Thinking outside of the dike for habitat restoration and monitoring. *Estuaries* 27(2): 273-282.

Hood, W.G. 2007. Landscape allometry and prediction in estuarine and coastal ecology: linking landform scaling to ecological patterns and processes. *Estuaries and Coasts* 30:895-900.

Hood, W.G. 2014.Geographic variation in Puget Sound tidal channel geometry – Developing a tool for restoration planning, design, and monitoring. Presentation at the Columbia River Estuary Workshop. May, 30, 2014 in Astoria, Oregon. Accessed 9/18/2015 at http://www.estuarypartnership.org/sites/default/files/resource_files/Hood_Columbia%20R%20workshop%202014%20Hood.pdf.

Howard, J., S. Hoyt, K. Isensee, M. Telszewski, and E. Pidgeon. 2014. Coastal blue carbon: methods for assessing carbon stocks and emissions factors in mangroves, tidal salt marshes, and seagrasses. Conservation International, Intergovernmental Oceanographic Commission of UNESCO, International Union for Conservation of Nature, Arlington, VA, USA.

Lindsay, J.B., and I.F. Creed. 2005. Removal of artifact depressions from digital elevation models: towards a minimum impact approach. *Hydrological Processes 19(6):3113-3126. doi:1* 0.1002/hyp.5835.

Meng, X., N. Currit, and K. Zhao. 2010. Ground filtering algorithms for airborne LIDAR data: A review of critical issues. *Remote Sensing* 2 (3): 833–60. doi:10.3390/rs2030833.

Metz, M., H. Mitasova, and R.S. Harmon. 2009. Fast stream extraction from large, radar-based elevation models with variable level of detail. Proceedings of Geomorphology 2009. Zurich, Switzerland. August 31 – September 2, 2009. Accessed 9/18/2015 at http://www.geomorphometry.org/system/files/metz2009geomorphometry.pdf.

Montané, J.M., and R. Torres. 2006. Accuracy assessment of LIDAR saltmarsh topographic data using RTK GPS. *Photogrammetric Engineering and Remote Sensing* 72 (8): 961–67. doi:0099-1112/06/7208–0961.

R Core Team. 2014. R: a language and environment for statistical computing. R Foundation for Statistical Computing, Vienna, Austria. URL http://www.R-project.org/.

Rosso, P.H., S.L. Ustin, and A. Hastings. 2006. Use of LIDAR to study changes associated with Spartina invasion in San Francisco Bay marshes. *Remote Sensing of Environment* 100 (3): 295–306.

Sadro, S., M. Gastil-Buhl, and J. Melack. 2007. Characterizing patterns of plant distribution in a southern California salt marsh using remotely sensed topographic and hyperspectral data and local tidal fluctuations. *Remote Sensing of Environment* 110 (2): 226–39. doi:10.1016/j.rse.2007.02.024.

Schmid, K.A., B.C. Hadley, and N. Wijekoon. 2011. Vertical accuracy and use of topographic LIDAR data in coastal marshes. *Journal of Coastal Research* 27 (6A): 116–32.

Shafer, D. J., and Yozzo, D. J. 1998. National guidebook for application of hydrogeomorphic assessment of tidal fringe wetlands. Technical Report WRP-DE-16, U.S. Army Engineer Waterways Experiment Station, Vicksburg, MS. Accessed 9/28/15 at http://el.erdc.usace.army.mil/elpubs/pdf/wrpde16.pdf.

So, K., S. van de Wetering, R. Van Hoy, and J. Mills. 2009. An analysis of reference tidal channel plan form characteristics for the Ni-les'tun Unit Restoration. February 2009 draft, US Fish and Wildlife Service, Confederated Tribes of Siletz Indians, Ducks Unlimited and NOAA.

Statewide Land Surveying Inc. 2012. Youngs and Wallooski River Survey Data Collection Report. Prepared for Cascade Environmental Group, LLC. Statewide Land Surveying Inc., Gresham, OR. 12 pp.

Tarboton, D.G. 1997. A new method for the determination of flow directions and upslope areas in grid digital elevation models. *Water Resources Research* 33(2): 309-319.

Wang, C., M. Menenti, M.P Stoll, A. Feola, E. Belluco, and M. Marani. 2009. Separation of ground and low vegetation signatures in LIDAR measurements of salt-marsh environments. *IEEE Transactions on Geoscience and Remote Sensing* 47 (7): 2014–23. doi:10.1109/TGRS.2008.2010490.

Watershed Sciences, Inc. 2009. LIDAR remote sensing data collection, Department of Geology and Mineral Industries (DOGAMI), North Coast, Oregon. Submitted to Oregon DOGAMI, Portland, OR. Watershed Sciences, Portland, OR.

Wehr, A., and U. Lohr. 1999. Airborne laser scanning—an introduction and overview. *ISPRS Journal of Photogrammetry and Remote Sensing* 54 (2-3): 68–82. doi:10.1016/S0924-2716(99)00011-8.

Wheatcroft, R. A. and C. K. Sommerfield. 2005. River sediment flux and shelf sediment accumulation rates on the Pacific Northwest margin. *Continental Shelf Research* 25(3): 311-332.

Williams, P.B., M.K. Orr, and N.J. Garrity. 2002. Hydraulic geometry: A geomorphic design tool for tidal marsh channel evolution in wetland restoration projects. *Restoration Ecology*, 10(3), 577–59.